

United Aircraft Research Laboratories



EAST HARTFORD, CONNECTICUT

D-910091-5

Experimental Investigation of the
Effect of Peripheral-Wall
Injection Technique on Turbulence
in an Air Vortex Tube

NASA Contract No. NASw-847

REPORTED BY David J. McFarlin
David J. McFarlin

APPROVED BY William M. Foley
William M. Foley
Chief, Aerophysics Section

DATE September 1965

NO. OF PAGES 45

COPY NO. 23

FOREWORD

An exploratory experimental and theoretical investigation of gaseous nuclear rocket technology is being conducted by the United Aircraft Corporation Research Laboratories under Contract NASw-847 with the joint AEC-NASA Space Nuclear Propulsion Office. The Technical Supervisor of the Contract for NASA is Captain W. A. Yingling (USAF). Results of the investigation conducted during the period between September 15, 1964 and September 15, 1965 are described in the following eleven reports (including the present report) which comprise the required third Interim Summary Technical Report under the Contract:

1. McFarlin, D. J.: Experimental Investigation of the Effect of Peripheral Wall Injection Technique on Turbulence in an Air Vortex Tube. UAC Research Laboratories Report D-910091-5, September 1965. (Unclassified)(present report)
2. Johnson, B. V.: Analytical Study of Propellant Flow Requirements for Reducing Heat Transfer to the End Walls of Vortex-Stabilized Gaseous Nuclear Rocket Engines (U). UAC Research Laboratories Report D-910091-6, September 1965. (report classified Confidential)
3. Travers, A.: Experimental Investigation of Peripheral Wall Injection Techniques in a Water Vortex Tube. UAC Research Laboratories Report D-910091-7, September 1965. (Unclassified)
4. Johnson, B. V., and A. Travers: Analytical and Experimental Investigation of Flow Control in a Vortex Tube by End-Wall Suction and Injection (U). UAC Research Laboratories Report D-910091-8, September 1965. (report classified Confidential)
5. Mensing, A. E., and J. S. Kendall: Experimental Investigation of the Effect of Heavy-to-Light-Gas Density Ratio on Two-Component Vortex Tube Containment Characteristics (U). UAC Research Laboratories Report D-910091-9, September 1965. (report classified Confidential)
6. Krascella, N. L.: Theoretical Investigation of the Opacity of Heavy-Atom Gases. UAC Research Laboratories Report D-910092-4, September 1965. (Unclassified)
7. Kesten, A. S., and R. B. Kinney: Theoretical Effect of Changes in Constituent Opacities on Radiant Heat Transfer in a Vortex-Stabilized Gaseous Nuclear Rocket (U). UAC Research Laboratories Report D-910092-5, September 1965. (report classified Confidential)

8. Marteney, P. J., N. L. Krascella, and W. G. Burwell: Experimental Refractive Indices and Theoretical Small-Particle Spectral Properties of Selected Metals. UAC Research Laboratories Report D-910092-6, September 1965. (Unclassified)
9. Williamson, H. A., H. H. Michels, and S. B. Schneiderman: Theoretical Investigation of the Lowest Five Ionization Potentials of Uranium. UAC Research Laboratories Report D-910099-2, September 1965. (Unclassified)
10. McLafferty, G. H., H. H. Michels, T. S. Latham, and R. Roback: Analytical Study of Hydrogen Turbopump Cycles for Advanced Nuclear Rockets. UAC Research Laboratories Report D-910093-19, September 1965. (Unclassified)
11. McLafferty, G. H.: Analytical Study of the Performance Characteristics of Vortex-Stabilized Gaseous Nuclear Rocket Engines (U). UAC Research Laboratories Report D-910093-20, September 1965. (report classified Confidential)

Experimental Investigation of the Effect of Peripheral-Wall
Injection Technique on Turbulence in an Air Vortex Tube

TABLE OF CONTENTS

	<u>Page</u>
SUMMARY	1
RESULTS	2
INTRODUCTION	3
DESCRIPTION OF EQUIPMENT AND PROCEDURES	4
Test Equipment and Installation	4
Test and Data Reduction Procedures	6
Test Conditions	7
DISCUSSION OF RESULTS	8
Results for Single-Slot Injection Configuration	8
Results for 2144-Port Injection Configuration	10
Comparison of Results for Single-Slot and 2144-Port Injection Configurations	11
REFERENCES	14
LIST OF SYMBOLS	15
FIGURES	17

Experimental Investigation of the Effect of Peripheral-Wall

Injection Technique on Turbulence in an Air Vortex Tube

SUMMARY

13835

Experiments were conducted to investigate the effect of the peripheral-wall injection technique used to drive an air vortex on the level of turbulence in the vortex. Two injection configurations were tested in separate 10-in.-dia vortex tubes. In one configuration, air was injected tangentially through a single 0.182-in.-high slot which extended along the entire 30-in. length of the tube. In the second configuration, air was injected approximately tangentially through 2144 ports of 0.060-in. dia distributed over the surface of the peripheral wall. In both tubes, a controlled quantity of air was removed through ports located at the centers of the two end walls or was injected through a porous tube located on the centerline of the vortex; air was also removed through perforated plates in the peripheral wall. Hot-wire-anemometer measurements of tangential velocity profiles and root-mean-square velocity fluctuations were made near the peripheral wall at three circumferential stations at one axial location (the axial midplane).

The results indicated that the interior region of low-turbulence flow was larger for the 2144-port configuration than for the single-slot configuration. This was primarily because the turbulent peripheral wall boundary layer was thinner for the 2144-port configuration.

author

RESULTS

1. For both injection configurations at small and intermediate positive values of radial Reynolds number (a measure of the net quantity of flow passing toward the centerline of the vortex tube), the turbulence intensity (the rms value of fluctuating velocity as a percentage of the local tangential velocity) decreased from values of 4% to 10% in the peripheral-wall boundary layer to values of less than 2% in the central flow region out of the boundary layer.

2. For small and intermediate positive radial Reynolds numbers, the volume of the central flow region in which the turbulence intensity was less than 2% was substantially larger for the 2144-port configuration than for the single-slot configuration.

3. For both injection configurations at zero and negative values of the radial Reynolds number, the absolute rms value of the fluctuating velocity decreased with decreasing radius. However, because of the rapid decrease of tangential velocity with decreasing radius, the turbulence intensity decreased much less than at positive radial Reynolds numbers, and in some cases it increased substantially.

4. The differences in turbulence intensity between the 2144-port and single-slot configurations at a given radius were substantially less at zero and negative radial Reynolds numbers than at intermediate positive radial Reynolds numbers.

5. The wavelength for maximum energy per unit wave number near the peripheral wall was approximately 1.0 in. for the single-slot configuration and approximately 0.1 in. for the 2144-port configuration.

INTRODUCTION

Gaseous nuclear rockets are potentially capable of providing values of specific impulse of 2000 to 3000 sec with thrust-to-weight ratios greater than unity. However, these performance capabilities will result in an economically attractive engine only if the nuclear fuel loss rates can be reduced substantially below the loss rates which would result from complete mixing of the fuel and propellant. Many different gaseous nuclear rocket concepts, designed to minimize fuel loss rate, have been proposed including some which are based on the suspension of gaseous nuclear fuel in a vortex. In all of these concepts, the fuel loss rates will be acceptably low only if the turbulence within the vortex is low.

The only known direct measurements of the turbulence within a vortex tube for different peripheral-wall injection techniques are reported in Ref. 1. In the configuration studied in Ref. 1, all of the flow injected into the vortex tube was removed through ports at the centers of the two end walls. However, studies conducted at the United Aircraft Research Laboratories (Ref. 2) have indicated that the turbulence which exists at intermediate radii in a vortex tube is reduced if the flow passing through the ports at the centers of the end walls is less than the total flow injected into the vortex tube, i. e., if a portion of the total flow injected is removed through the peripheral wall. In addition, dye photographs taken during the tests of Ref. 2 indicate that the turbulence is less if the flow is injected through a large number of small ports than if the flow is injected through a single slot.

The objective of the investigation reported herein was to experimentally determine the levels of turbulence associated with two different peripheral-wall injection techniques when the flow removed from the centers of the end walls was substantially less than the flow injected through the peripheral wall.

DESCRIPTION OF EQUIPMENT AND PROCEDURES

Test Equipment and Installation

Vortex Tubes

Two air vortex tubes with different peripheral-wall injection configurations were used (Figs. 1 and 2). Both vortex tubes were driven by the injection of air in essentially a tangential direction along the wall through the two different injection geometries.

A sketch showing the geometry of the vortex tube with single-slot injection is presented in Fig. 1. The vortex tube consisted of a cylindrical metal tube, 10 in. in diameter and 30 in. in length. Air was injected through a 0.182 \pm 0.005-in.-high injection slot extending the entire length of the tube. A controllable quantity of air was withdrawn through a bypass exhaust screen located in the peripheral wall just upstream of the injection slot. In most tests the remaining flow, designated the thru-flow, was withdrawn through ports at the centers of the end walls. In some tests, flow was injected into the vortex tube through a porous tube located on the centerline. An end-view photograph of the vortex tube with one end wall removed is shown in Fig. 3a. Figure 3b is a photograph of the vortex tube assembly with the end walls attached.

A sketch showing the geometry of the vortex tube with 2144-port injection is shown in Fig. 2. This vortex tube consisted of a cylindrical lucite tube, also with a diameter of 10 in. and a length of 30 in. Four 1.5-in.-wide lucite channels were attached to the outside of the tube to form peripheral bypass plenums for the bypass flow. The 10-in.-dia tube was mounted concentrically inside another lucite tube which was 14 in. in inside diameter and 30 in. in length, and which served as an injection plenum chamber. A total of 2144 injection ports, 0.060-in. in diameter, were located in 119 staggered circumferential rows 0.25 in. apart. The centerline of each injection port was at an angle of 19 deg relative to a tangent to the inner wall of the vortex tube. As in the case of the single-slot configuration, most of the injected air was withdrawn through the four peripheral bypass exhaust screens. The remaining flow was withdrawn through the thru-flow ports in the end walls in the same manner as for the single-slot vortex tube. Figure 4 is a photograph of the 2144-port vortex tube. A detailed description of the 2144-port configuration is contained in Ref. 2.

The same end walls were used with both the single-slot injection and the 2144-port injection vortex tubes. They were smooth lucite discs with a 1-in.-dia hole in the center for the removal of the thru-flow. The end-wall thru-flow ports permitted

amounts of radial inflow to be controlled independent of the amount of injected flow. For radial outflow tests a porous tube was mounted on the vortex tube centerline and extended the full length of the vortex tube. The injection tube consisted of a 0.5-in.-dia metal cylinder containing a large number of 0.125-in.-dia holes which were covered by multiple layers of fiberglas cloth to ensure an approximately uniform outflow of air along the length of the tube.

Test Installation

The bypass and thru-flow lines were connected to a vacuum system and room air was drawn through the vortex tube. The vacuum pump was located approximately 100 ft from the test rig so that any fluctuations in pressure level due to the pump were damped out. The bypass and thru-flow weight flows were measured with standard A.S.M.E. long-radius flow nozzles. A Cambridge Absolute Filter, which removes at least 99.98% of all particles greater than 0.1 micron, was positioned in the inlet of the vortex tube injection manifold to reduce the possibility of hot-wire breakage caused by particulate matter in the room air and to reduce dust collection on the wire.

Hot-Wire Anemometer

The velocity and turbulence intensity measurements were made using constant-temperature hot-wire anemometers. A Thermo-Systems, Inc. Model 1010 Constant-Temperature Anemometer was used for the measurements in the single-slot vortex tube, and a Disa Elektronik A/S Constant-Temperature Anemometer was used for the measurements in the 2144-port tube. Both units have similar operating characteristics and the accuracy of both is limited to the accuracy of the anemometer bridge voltmeter. When operated with a 0.15-mil-dia tungsten wire the maximum frequency response is approximately 50,000 cps, and the output noise level was observed to be less than 0.8 mv rms.

Both anemometers had d-c voltmeters built into their circuits. The voltage reading error was $\pm 2\%$ with the Thermo-Systems, Inc. unit and less than $\pm 1\%$ with the Disa unit. The a-c voltages were measured externally with a Ballantine True Root-Mean-Square Voltmeter. A Magnacorder Model 728 two-channel tape recorder, with a flat response between 50 cps and 3000 cps, was used to record turbulence intensity spectra. A General Radio Type 1900-A Wave Analyzer was used to analyze the frequency data on the magnetic tapes.

Figure 5 shows a typical hot-wire probe used in this study. The probes were modified Thermo-Systems, Inc. type N.T.-28 Boundary Layer Sensors. They were 0.062 in. in diameter and 6 in. in length. The sensor (hot) wires were of tungsten and were 0.15 mil in diameter and 0.045 in. in length. The wires were offset from the centerline of the probe by 0.25 in. to minimize the effects of the longitudinal

boundary layer along the probe (flow induced by the radial pressure gradient in the vortex flow field).

Test and Data Reduction Procedures

For both vortex tube injection configurations, the desired airflow condition was specified in terms of the injection and radial Reynolds numbers. The injection Reynolds number

$$Re_{t,j} = \frac{\rho V_j r_l}{\mu} = \frac{\dot{W} r_l}{A_j \mu g} \quad (1)$$

was established by setting the injection air weight flow, \dot{W} . The radial Reynolds number (sometimes called the thru-flow Reynolds number, $Re_{r,t}$, e.g., Ref. 2)

$$Re_r = \frac{\dot{W}_{TF}}{2\pi\mu g L} \quad (2)$$

was established independently by setting the thru-flow weight flow, \dot{W}_{TF} .

The conventional heat transfer relation for a cylinder in crossflow, as applied to heated wires, is (from Ref. 3)

$$Nu \left(\frac{T_s}{T_e} \right)^{-0.17} = C + D Re^{0.5} \quad (3)$$

Rewriting Eq. (3) in terms of the output of the hot-wire anemometer gives

$$\frac{E^2}{R} = \left(A + B \sqrt{\frac{g \rho u}{\mu}} \right) (T_s - T_e) \quad (4)$$

where A and B are constants determined by calibration. Equation (4) indicates that the square of the d-c voltage output of the anemometer is proportional to the square root of the product of the fluid density and velocity when the fluid temperature and viscosity are held constant. Figure 6 shows a typical calibration curve. The departure of the calibration data points from the straight line (from Eq. (4)) is sufficient to cause measured velocity errors of twelve to fourteen percent. Since this investigation is concerned primarily with the shape of the velocity profiles rather than their absolute value, this accuracy was considered acceptable.

The turbulence intensity was calculated from the probe output voltage using the relation (from Ref. 4)

$$\frac{v'}{v_\phi} = \frac{4 E e}{E^2 - E_0^2} \quad (5)$$

and the fluctuating component of the turbulence intensity was obtained by multiplying Eq. (5) by the measured tangential velocity, v_ϕ . Since no calibration is required for the turbulence intensity as calculated by Eq. (5), these values are accurate to approximately 4% when the value of mean velocity is large relative to the value of fluctuating velocity. Large reading errors in mean velocity are introduced when the fluctuating velocity (a-c signal) and the mean velocity (d-c signal) are of the same order of magnitude due to the a-c signal being superimposed on the d-c signal.

The turbulence spectrum data were analyzed using a 10 cps bandwidth filter at a scanning rate of 0.3 cps/sec. The spectral data are presented in terms of wave number, defined as

$$K = \frac{2\pi f}{v_\phi} \quad (6)$$

and turbulent energy per unit wave number, defined as

$$F_{v'}(K) = \frac{v'^2 v_\phi}{2\pi f} \quad (7)$$

If the axis of the hot wire is not normal to the flow direction, the right side of Eq. (4) must be multiplied by a function of the sine of the angle between the axis of the hot wire and the direction of flow. Therefore, in order to ensure that the probe was aligned properly with the flow, it was always rotated until the anemometer bridge voltage reached a maximum.

Test Conditions

Radial profiles of velocity and turbulence in the single-slot vortex tube were obtained at three measuring stations located 90 deg apart around the tube. The first station (Measuring Station No. 1) was 30 deg downstream from the injection slot (see

Fig. 1). Profiles in the 2144-port vortex tube were taken at three measuring stations located in one quadrant of the tube as shown in Fig. 2. The first station (Measuring Station No. 1) was positioned midway between the downstream edge of the bypass screen and the first line of injection ports.

For both tubes, radial Reynolds number, Re_r , was varied from -26 (radial outflow) to 180 (radial inflow). If all of the flow injected through the peripheral wall had been withdrawn through the thru-flow duct, the radial Reynolds number would have been 1170. The injection Reynolds number was held constant at $Re_{t,j} = 1.9 \times 10^5$ for the single-slot vortex tube and at $Re_{t,j} = 2.2 \times 10^5$ for the 2144-port vortex tube.

It was observed from dye patterns in water vortex tests of the type described in Ref. 2 that, when probing radially into the flow from the peripheral wall, a radial inflow boundary layer formed along the length of the probe. This effect appeared when the probe was inserted into the vortex a distance greater than about 0.75 in. to 1 in. from the peripheral wall. In the present investigation, the inflow boundary layer along the probe would cause the measured turbulence intensity to be higher than the actual value in the interior region of the vortex. Because the effect of the probe wake on the magnitude of the measurements is not known, few data (except for the radial outflow case) were taken at radii less than 4.0 in. where this wake effect will be most important. In the radial outflow case the measurements are not affected as severely because the radial pressure gradient is too small to cause the probe wake to fall radially inward into the vicinity of the hot wire.

DISCUSSION OF RESULTS

Results for Single-Slot Injection Configuration

The effects of radial Reynolds number on the tangential velocity profiles at Measuring Station Nos. 1, 2 and 3 are shown in Figs. 7, 8 and 9, respectively. The general increase in the level of the tangential velocities towards the center of the tube with increasing radial Reynolds number indicates increasing vortex strength, i.e., flow conditions approaching those of a true vortex ($V_\phi \propto 1/r$). In Fig. 7 the persistence of the injection jet near the wall is apparent; the high-velocity region is only slightly thicker than the 0.182-in. injection slot height. At Station Nos. 2 and 3 (Figs. 8 and 9) the jet boundary layer has thickened relative to that for Station No. 1. In the remaining portion of the vortex tube between Station No. 3 and the peripheral bypass screen, the boundary layer may grow thicker than it was at Station No. 3. For radial outflow, $Re_r = -26$ (Fig. 9), the tangential velocity decreases to approximately 2.5 ft/sec at $r = 3.0$ in. This result is consistent

with visual observations of dye patterns in vortex tubes which for this flow condition indicate a vortex core region of very low tangential velocity (Ref. 2).

The corresponding effects of radial Reynolds number on the turbulence intensity profiles at Station Nos. 1, 2 and 3 are shown in Figs. 10, 11 and 12, respectively. Note in Fig. 10 that the turbulence level is high near the peripheral wall but decreases with radial distance inward. For radial inflow (i.e., radial Reynolds number greater than 0), the turbulence level decreases to approximately 1.5% at a distance of 1.0 in. from the peripheral wall, while it stabilizes at approximately 4% for a radial Reynolds number of 0. Note that the peak in the percent turbulence curve occurs at approximately $r = 4.75$ in., which is near the inner edge of the boundary layer (see Fig. 7). Proceeding from this peak toward the peripheral wall, the percent turbulence decreases as the velocity increases toward the peak of the jet (Fig. 7).

Figure 11 shows the effect of radial Reynolds number on the turbulence intensity at Station No. 2. Very close to the peripheral wall the turbulence is approximately twice its value at Station No. 1 (Fig. 10) but decreases very rapidly to 1.5% at $r = 4.0$ in. for cases with radial inflow ($Re_r > 0$). The percent turbulence for $Re_r = 0$ again stabilized between 4% and 5%. The turbulence intensity is high in the region near the wall at the outer edge of the boundary layer but shows no hump in the curve at the inner edge of the boundary layer.

Figure 12 shows similar turbulence intensity profiles at Station No. 3. For radial inflow the results at this station are similar to the results at Station No. 2. For radial outflow ($Re_r = -26$), the percent turbulence near the peripheral wall is approximately the same as for radial inflow and decreases with increasing distance from the wall until it is a minimum at $r = 4.40$ in.; it then increases to 13% at approximately $r = 3.5$ in. Note in the upper plot that the absolute value of the turbulence intensity decreases continually with increased distance from the peripheral wall for all Reynolds numbers. However, for radial outflow the fluctuating velocity at $r = 3.0$ in. is almost one-fifth as large as the tangential velocity (Fig. 9) so that large experimental errors might exist for these data points (see Test and Data Reduction Procedures section).

Figure 13 shows a comparison of the turbulence intensity profiles at Station Nos. 1, 2 and 3 at a radial Reynolds number of 100. These curves illustrate the effect of distance downstream of the injection slot on the turbulence level. Very close to the peripheral wall the turbulence level increases with downstream distance. As distance from the peripheral wall increases, the turbulence level becomes relatively insensitive to downstream distance.

Figure 14 illustrates the effect of a change in radius close to the wall on the spectral distribution of turbulent energy. The solid curve is for $r = 4.875$ in.

and the dashed curve is for $r = 4.25$ in. Close to the peripheral wall the turbulent energy is concentrated in longer wavelengths than at a distance of 0.75 in. from the wall. According to Ref. 5, the longer wavelengths near the peripheral wall are probably due to elongation of the eddies caused by wall shear. Away from the wall the eddies are more spherical and consequently have a shorter wavelength in the direction of the mean flow. The wavelengths in which the energy of the eddies is concentrated at the inner radius of 4.25 in. are in the neighborhood of 0.2 in., which is approximately three probe diameters (Fig. 5). Hence it is possible that near the peak in this spectrum some of the indicated turbulence is caused by the probe wake.

Results for 2144-Port Injection Configuration

Figure 15 shows the effects of radial Reynolds number on the tangential velocity profiles at Station No. 1. Note that the boundary layer at this station is very thin due to the removal of a portion of the boundary layer by the peripheral bypass screen just upstream of the measuring station and due to the distributed blowing. The effects of radial Reynolds number on the tangential velocity profiles at Station Nos. 2 and 3 are shown in Figs. 16 and 17, respectively. The total boundary layer thickness shown in Figs. 15 through 17 are considerably smaller than those for single-slot injection shown in Figs. 7 through 9. Again, as in the case of the single-slot injection configuration, the tangential velocity profile for radial outflow ($Re_r = -26$; Fig. 16) drops to approximately 2.5 ft/sec at $r = 3.0$ in., indicating the existence of a core region of very low tangential velocity which has been observed in dye patterns in water-vortex flows (Ref. 2).

The effect of radial Reynolds number on the turbulence intensity profiles at Station No. 1 is shown in Fig. 18. The turbulence level for radial inflow is approximately 4.5% near the peripheral wall but decreases rapidly to 1.5% with radial distance inward. For $Re_r = 0$, the percent of turbulence is approximately constant at 4% outside $r = 4.0$ in. but increases at radii less than $r = 4.0$ in. This general behavior is similar to that observed for the single-slot injection configuration (Figs. 10, 11 and 12). The turbulence level at Station No. 2 (Fig. 19) is very high adjacent to the peripheral wall but decreases very rapidly to approximately 0.5% at $r = 4.2$ in. For $Re_r = 0$ the turbulence profile is approximately the same as for Station No. 1 except within 0.2 in. of the peripheral wall where the turbulence level is higher. For radial outflow ($Re_r = -26$), the percent turbulence is over 11% near the peripheral wall and decreases with increased distance from the wall to $r = 4.2$ in., where it is a minimum, and then increases to 12% at $r = 3.25$ in. Note that the absolute value of the turbulence intensity decreases continually with increased distance from the peripheral wall as it did for the single-slot configuration. Again, it should be noted that the possibility of experimental error is increased when the value of the fluctuating velocity approaches the value of the tangential velocity as it does in the low-velocity core region for $Re_r < 0$ (see Test and Data Reduction Procedures section).

Figure 20 shows the effect of radial Reynolds number on the turbulence intensity at Station No. 3. Close to the peripheral wall, the percent turbulence is approximately 6.5%, which is almost half the corresponding value at Station No. 2. For $r < 4.25$ in., the turbulence profiles at all Reynolds numbers are similar to the corresponding profiles at Station Nos. 1 and 2.

Figure 21 shows a comparison of the turbulence intensity profiles at Station Nos. 1, 2 and 3 for a radial Reynolds number of 100. The curves illustrate the effect of downstream distance along the peripheral wall on turbulence level. Near the peripheral wall, the turbulence level increases from Station No. 1 to Station No. 2, and then decreases slightly to Station No. 3, which is immediately downstream of an injection port. Further from the peripheral wall the turbulence level is relatively insensitive to downstream distance.

The effect of radial position on the spectral distribution of turbulent energy is shown in Fig. 22. Radial position has very little effect on the wavelength for maximum energy concentration, although the radial Reynolds number does affect the absolute intensity. At $r = 4.75$ in. the peak energy occurs at a wavelength of approximately 0.1 in., and at $r = 4.25$ in. the peak has shifted slightly to approximately 0.06 in.

Comparison of Results for Single-Slot and 2144-Port Injection Configurations

Figure 23 shows a comparison of the tangential velocity profiles at Station Nos. 1, 2 and 3 for the single-slot and the 2144-port injection configurations. For the single-slot configuration the thickness of the peripheral-wall boundary layer increases with increased circumferential distance from the injection slot so that at Station No. 3 the boundary layer occupies approximately the outer 0.5 in. of the tube. In the remaining circumferential distance between Station No. 3 and the peripheral bypass screen, the boundary layer would be expected to thicken considerably. It can be seen that the fraction of the vortex tube occupied by the peripheral-wall boundary layer is considerably smaller for the 2144-port injection configuration than for the single-slot configuration.

Figure 24 shows averages of the percent turbulence corresponding to the flow conditions of Fig. 23 for the two vortex injection configurations. These curves are based on arithmetic averages of the measurements at the three measuring stations in each tube. It should be pointed out that the curve for the single-slot injection configuration is probably lower than the true average for the entire tube because no measurements were made around nearly half of the circumference of the vortex tube (between Station No. 3 and the peripheral bypass screen; see sketch in Fig. 23).

Hence, the thickest portion of the boundary layer was not included in the averaging process. The curve for the 2144-port configuration is a good indication of the true average turbulence in the tube because the measuring stations cover a large percentage of a representative quadrant. The curves are dashed near the peripheral wall because of the uncertainty of averaging in the region of the boundary layer. It can be seen in Fig. 24 that the 2144-port configuration was considerably less turbulent than the single-slot configuration throughout the region surveyed.

The effect of radial Reynolds number on the tangential velocity at $r = 4.5$ in. is shown in Fig. 25. The large difference between the curves at Station Nos. 1 and 2 and Station No. 3 for the single-slot injection configuration is caused by the thick boundary layer extending inward to this radius at Station No. 3 for some Reynolds numbers. The curves for the 2144-port configuration are not significantly different at the three measuring stations because the boundary layer does not extend inward to $r = 4.5$ in. (see Fig. 23). Figure 26 shows average percent turbulence data at $r = 4.5$ in. for the same flow conditions as in Fig. 25. At this radius, injection technique shows a strong effect on the turbulence level for radial Reynolds numbers larger than 25; at these radial Reynolds numbers the 2144-port configuration is markedly less turbulent than the single-slot configuration. Again, it should be noted that the curve for the single-slot configuration was averaged in the same manner as for Fig. 24 so that the turbulence values shown are probably lower than the true average for the entire tube.

Figure 27 shows a comparison of the energy spectra for the single-slot and 2144-port configurations at Station No. 2 and a radius of 4.75 in. The wavelength of maximum energy shifted from approximately 1 in. for the single-slot configuration to approximately 0.1 in. for the 2144-port configuration. This difference in turbulence spectrum would have a correspondingly large influence on the turbulent transport properties of the flow. This apparently accounts for the major differences in dye patterns reported in Ref. 2 for these two injection configurations.

Figure 28 shows a comparison of typical tangential velocity profiles for the two injection configurations at a radial outflow Reynolds number of -26. The boundary layer for the single-slot configuration is approximately twice as thick as for the 2144-port configuration. Note that the tangential velocity is very nearly zero at $r = 2.5$ in. This result is consistent with flow-visualization tests of these configurations (Ref. 2) which have indicated the existence of an inner region of very low tangential velocity. The turbulence intensities for this radial outflow condition are compared in Fig. 29. These curves show less influence of injection technique on turbulence level than for radial inflow. It appears that for radial outflow a larger fraction of the total turbulence is determined by the interior region of the vortex flow, compared with its contribution for radial inflow.

In summary, for radial inflow, the volume of flow with a turbulence level less than 2% was substantially larger for the 2144-port injection configuration than for the single-slot configuration. Perhaps more important, turbulence spectra indicate that the size of the eddies associated with the peak turbulence intensity are an order of magnitude smaller in the 2144-port configuration; this would be expected to result in lower values of eddy diffusivity and eddy viscosity for this configuration.

REFERENCES

1. Kendall, J. M., Jr.: Experimental Study of a Compressible Viscous Vortex. Jet Propulsion Laboratory Technical Report No. 32-290, June 5, 1962.
2. Travers, A.: Experimental Investigation of Peripheral-Wall Injection Techniques in a Water Vortex Tube. United Aircraft Research Laboratories Report D-910091-7, September 1965.
3. Collis, D. C. and M. J. Williams: Two-Dimensional Convection from Heated Wires at Low Reynolds Numbers. Journal of Fluid Mechanics, Vol. 6, 1959, p. 357.
4. Anon: Applications of the Heat Flux System in Low Temperature Gases and Liquids. Thermo-Systems, Inc. Technical Bulletin No. 4.
5. Hinze, J. O.: Turbulence. McGraw-Hill Book Company, Inc., New York, 1959, p. 440.

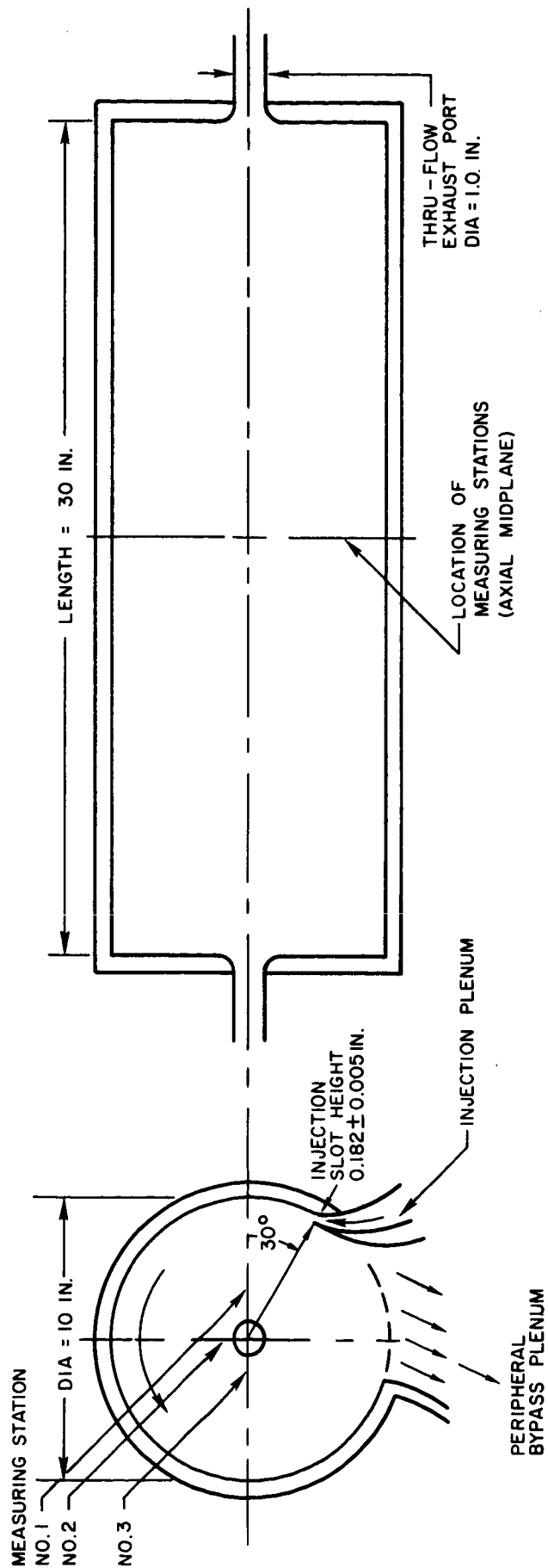
LIST OF SYMBOLS

A, B	Constants (Eq. (4))
A_j	Total area of injection slot or ports at peripheral wall, ft^2
C, D	Constants (Eq. (3))
d_w	Diameter of hot-wire, 0.15 mil
e	rms of fluctuating output of hot-wire anemometer, mv
E	Output of hot-wire anemometer, volts d-c
E_0	Output of hot-wire anemometer at zero velocity, volts d-c
$F_v(k)$	Turbulent energy per unit wave number, $\text{in.}^3/\text{sec}^2$
h	Heat transfer coefficient, $\text{Btu/hr-ft}^2\text{-deg F}$
f	Frequency of velocity fluctuation, cycles/sec
g	Gravitational constant, 32.2 ft/sec^2
k	Wave number, $(\text{in.})^{-1}$
k_f	Thermal conductivity of environment fluid, $\text{Btu/hr-ft}^2\text{-deg F}$
L	Length of vortex tube, 2.5 ft
Nu	Nusselt number, hd_w/k_f
r	Radius from center of vortex tube, in.
r_i	Radius of vortex tube, ft
R	Electrical resistance of hot-wire sensor, ohms
Re	Reynolds number, $\rho u d_w / \mu$
Re_r	Radial Reynolds number based on thru-flow weight flow, $\dot{W}_{TF} / 2\pi\mu gL$

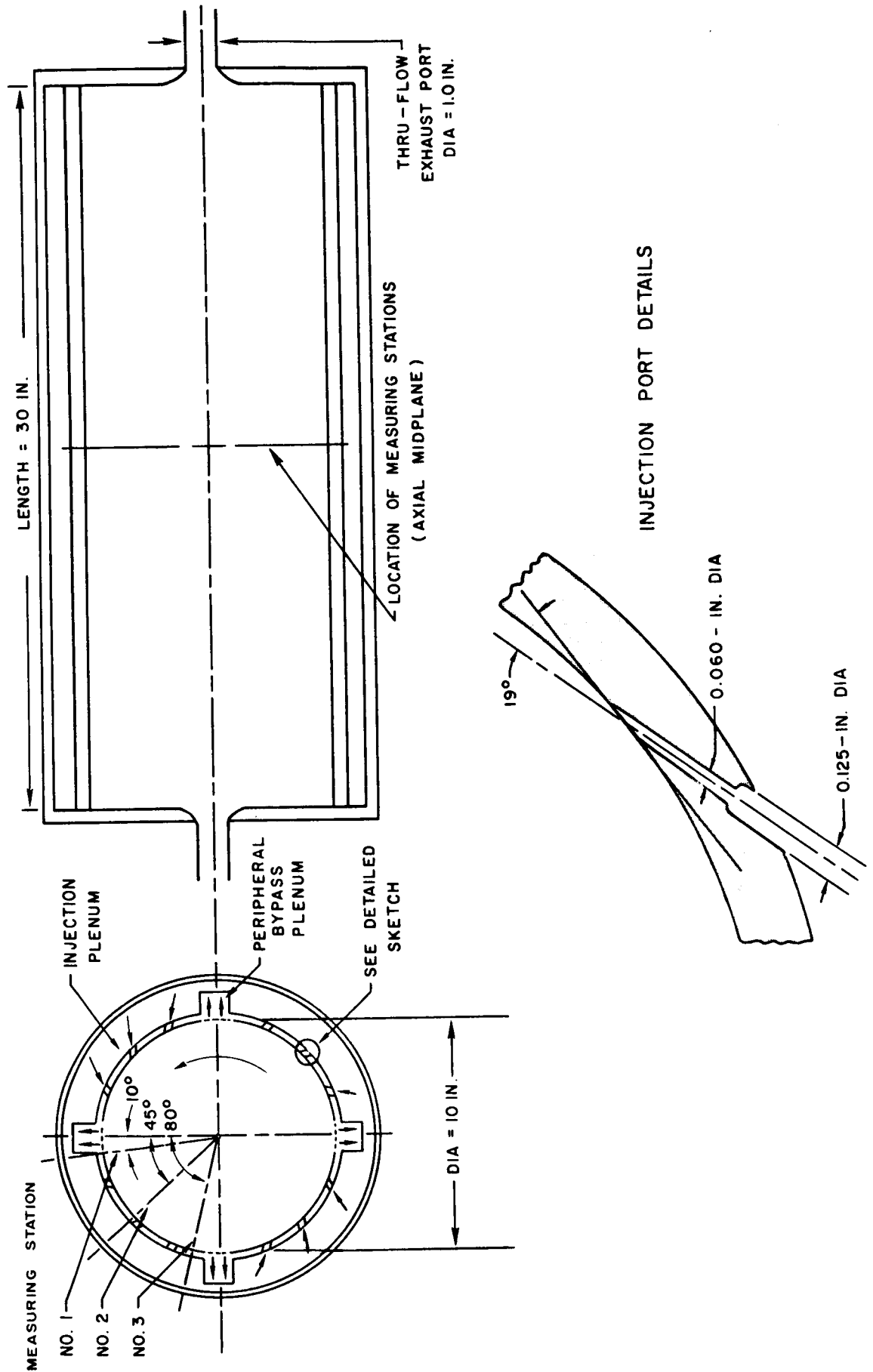
LIST OF SYMBOLS (Cont'd.)

$Re_{t,j}$	Injection Reynolds number based on average inlet jet velocity, $\rho v_j r_1 / \mu = \dot{W} r_1 / A_j \mu g$
T_e	Environment temperature, deg F
T_s	Surface temperature of hot-wire sensor, deg F
u	Velocity, ft/sec
v_j	Average injection jet velocity, $\dot{W} / g \rho A_j$ - ft/sec
v'	rms of fluctuating velocity, ft/sec
v_ϕ	Tangential component of velocity in primary flow, ft/sec
\dot{W}	Total weight flow injected through peripheral wall, lb/sec
\dot{W}_{TF}	Total thru-flow weight flow or weight flow injected through centerline porous injection tube, lb/sec
μ	Viscosity, lb-sec/ft ²
ρ	Density, slugs/ft ³

GEOMETRY OF VORTEX TUBE WITH SINGLE-SLOT INJECTION

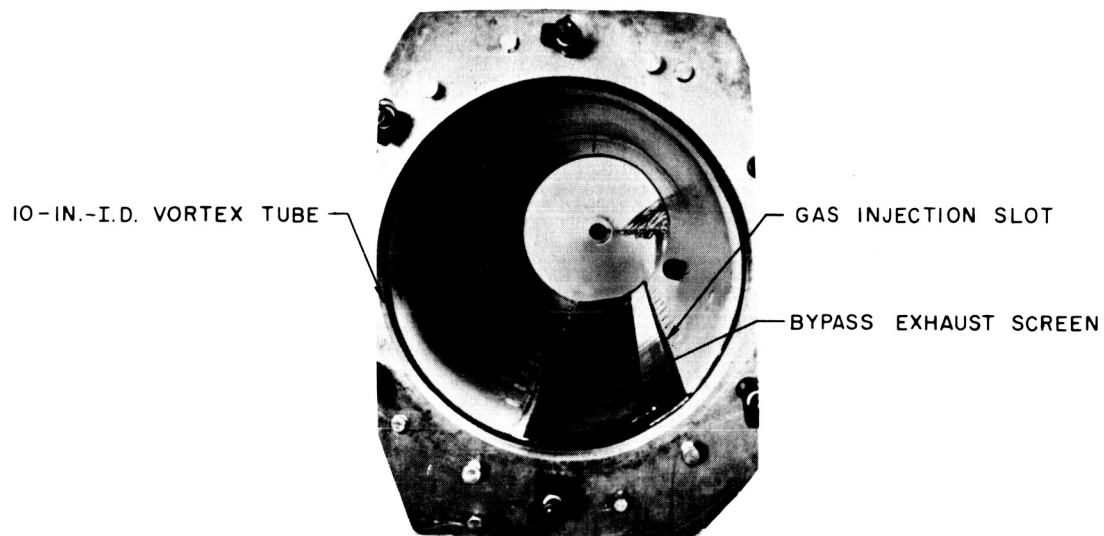


GEOMETRY OF VORTEX TUBE WITH 2144 - PORT INJECTION

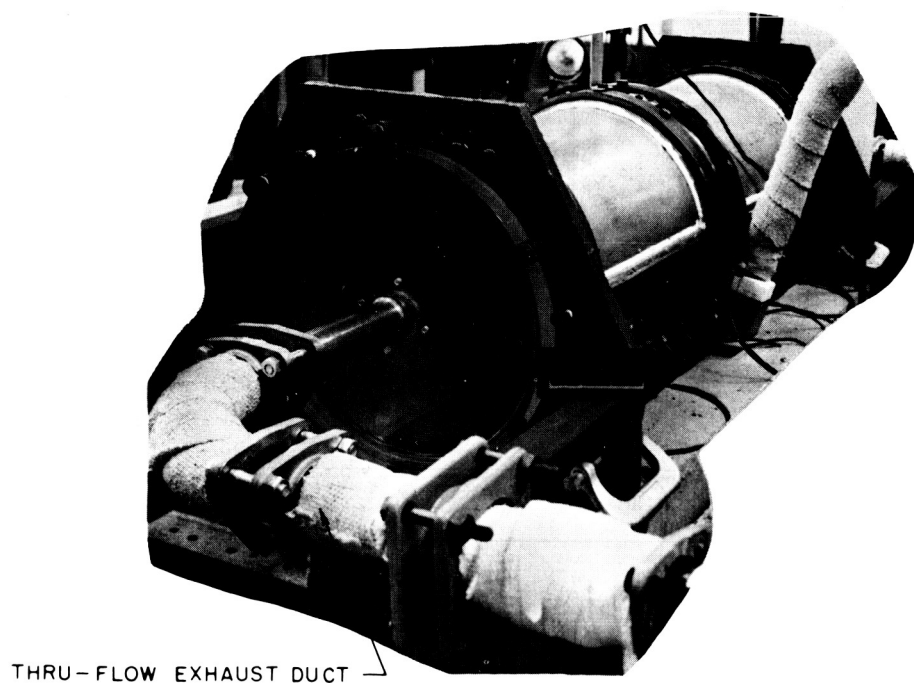


PHOTOGRAPHS OF VORTEX TUBE WITH SINGLE-SLOT INJECTION

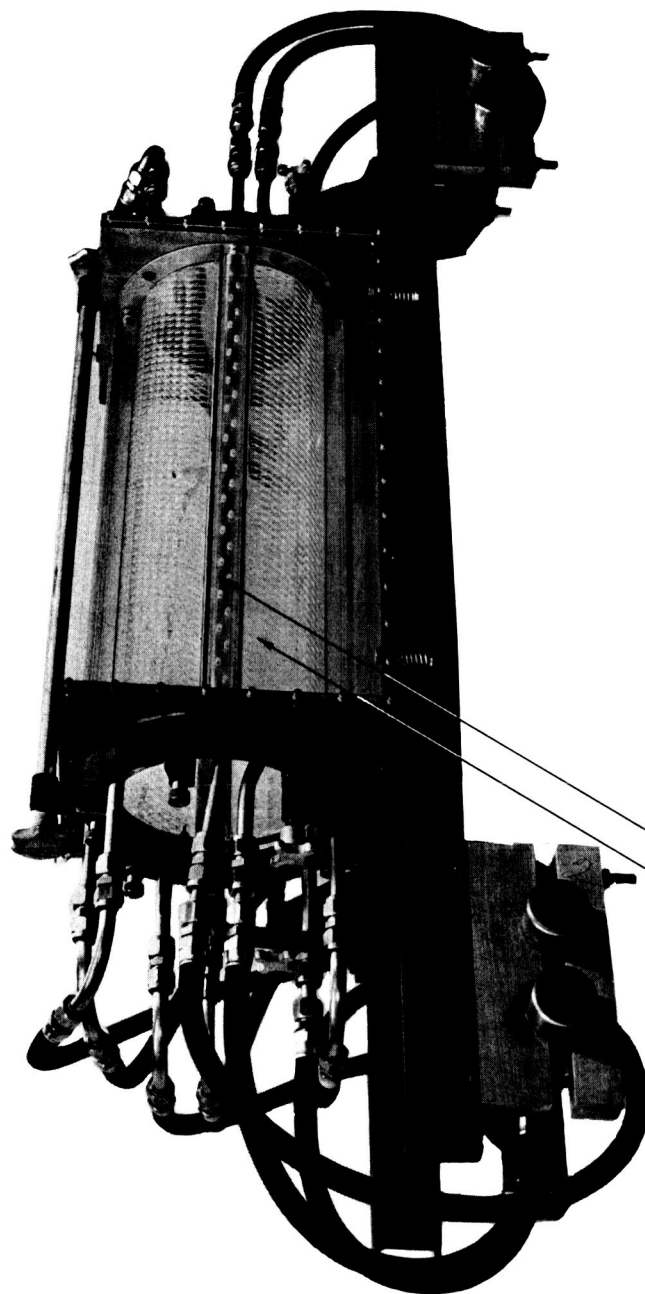
a. END VIEW WITH END WALL REMOVED



b. OVERALL VIEW



PHOTOGRAPH OF VORTEX TUBE WITH 2144 - PORT INJECTION

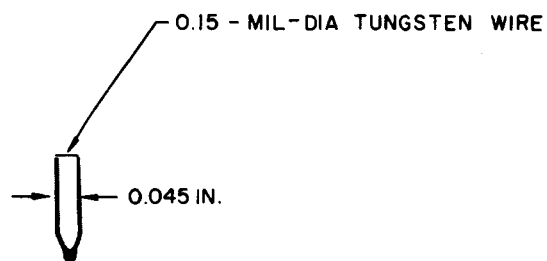


— PERIPHERAL BYPASS PLENUM

— 0.060 - IN.- DIA INJECTION PORTS

PHOTOGRAPHS OF HOT WIRE PROBE

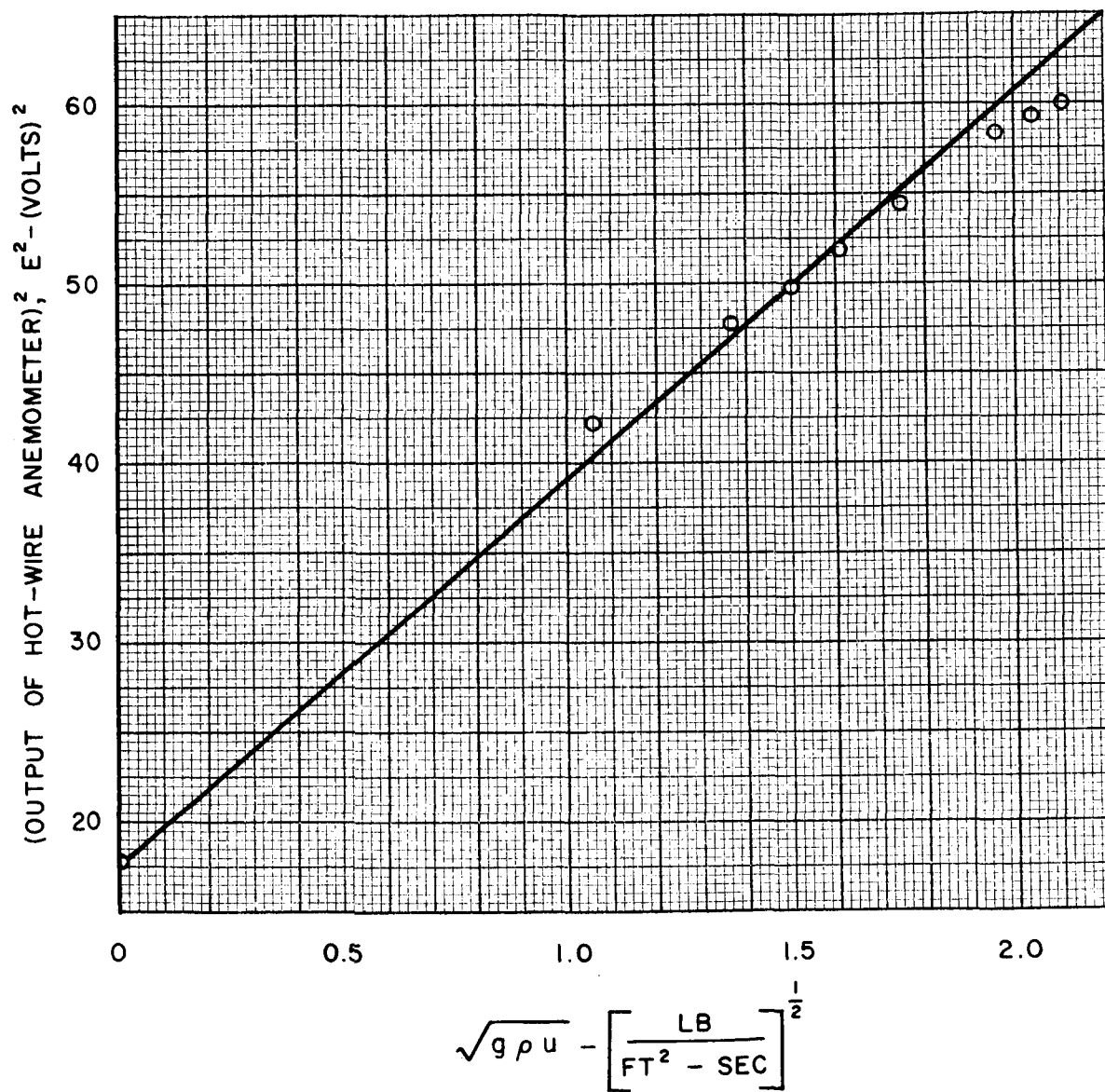
END VIEW



SIDE VIEW



TYPICAL HOT-WIRE ANEMOMETER CALIBRATION CURVE

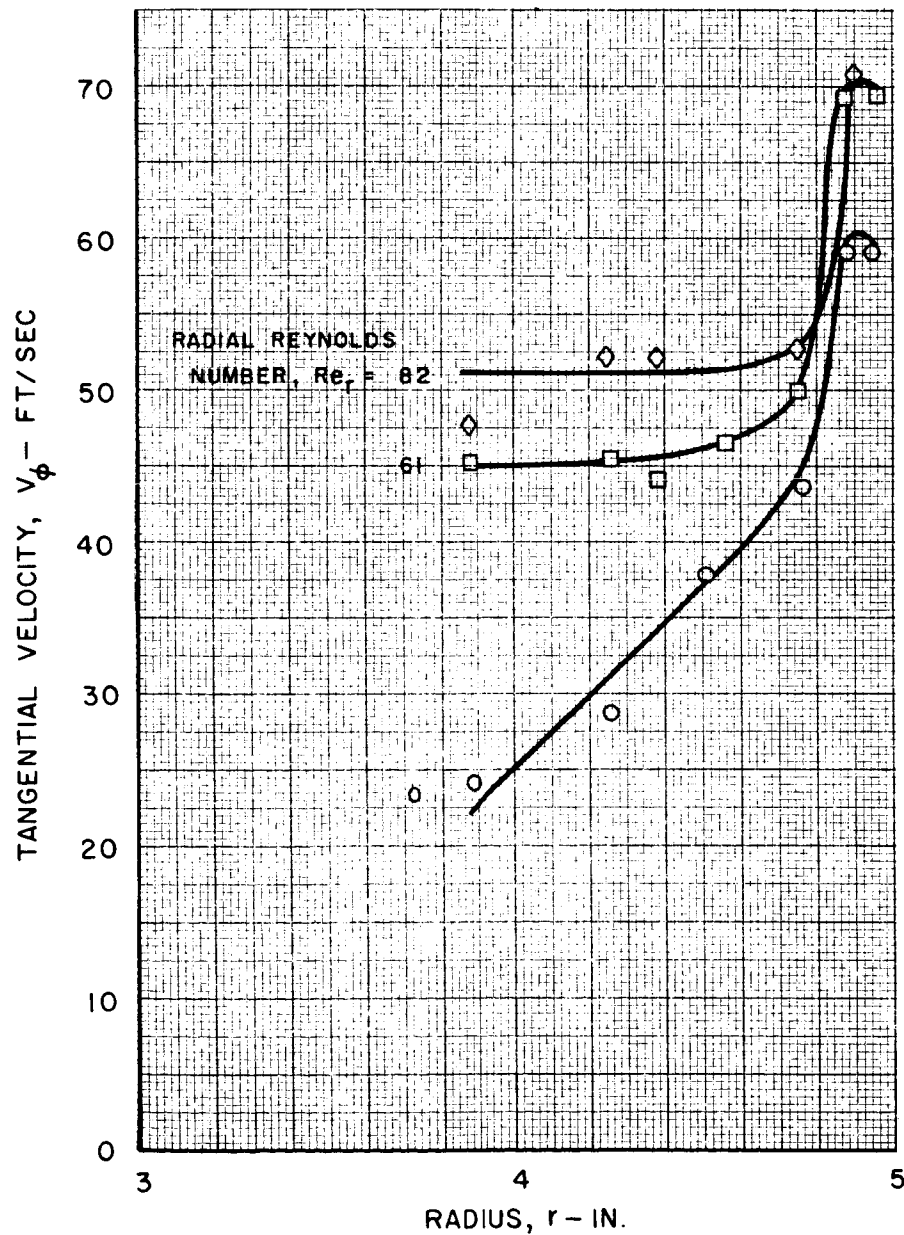
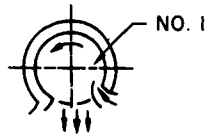


EFFECT OF RADIAL REYNOLDS NUMBER ON TANGENTIAL VELOCITY PROFILES AT STATION NO. I FOR SINGLE - SLOT INJECTION

JET REYNOLDS NUMBER, $Re_{t,j} = 1.9 \times 10^5$

JET VELOCITY, $V_j = 76$ FT/SEC

MEASURING STATION

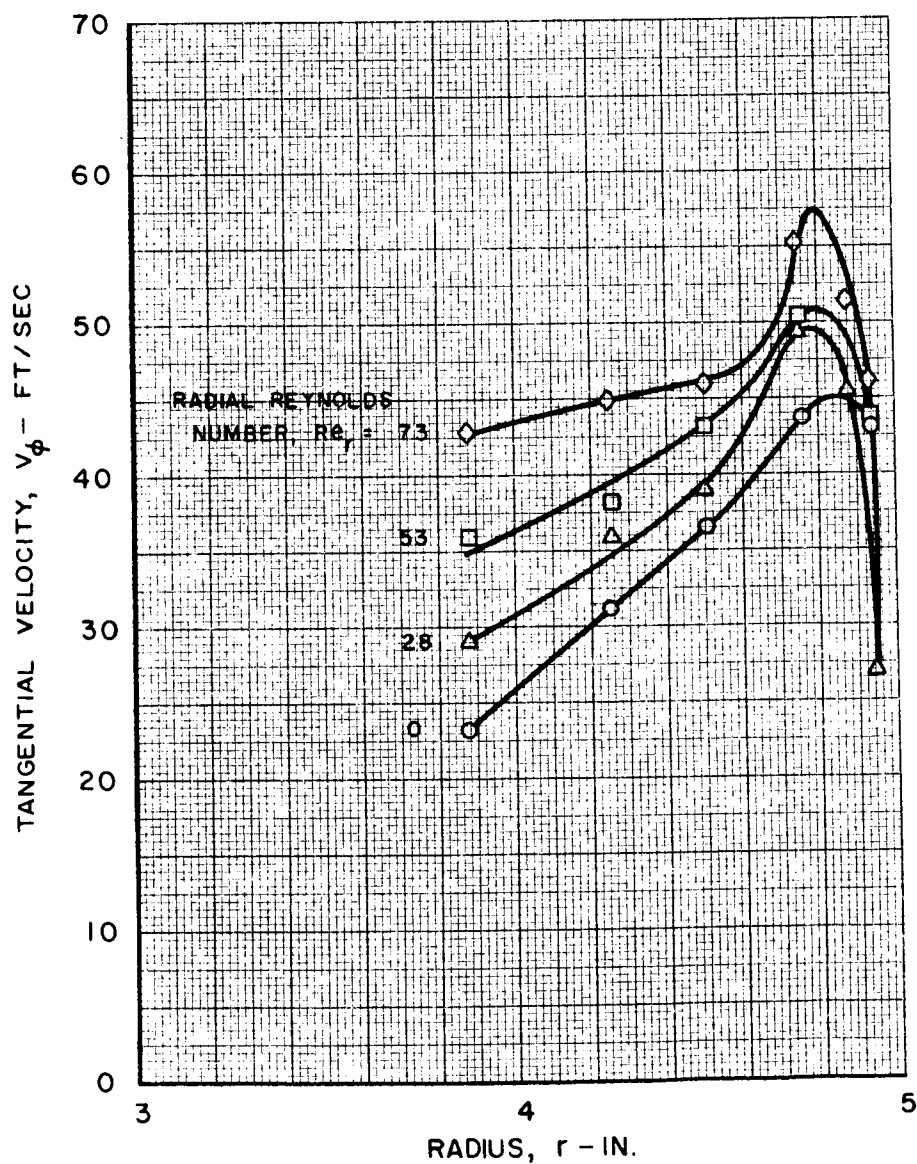


EFFECT OF RADIAL REYNOLDS NUMBER ON TANGENTIAL VELOCITY PROFILES AT STATION NO. 2 FOR SINGLE - SLOT INJECTION

JET REYNOLDS NUMBER, $Re_{t,j} = 1.9 \times 10^5$

JET VELOCITY, $V_j = 76$ FT/SEC

MEASURING STATION

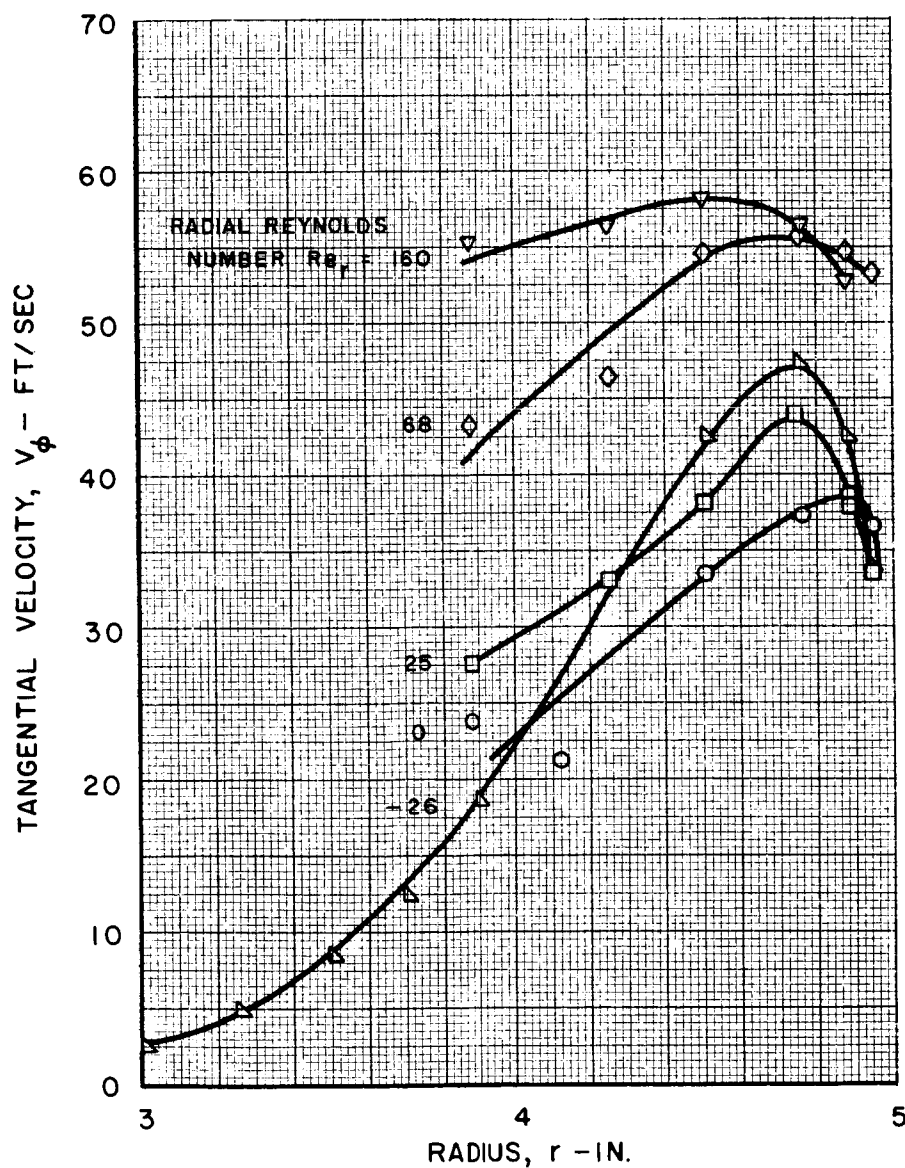
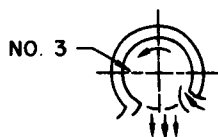


EFFECT OF RADIAL REYNOLDS NUMBER ON TANGENTIAL VELOCITY PROFILES AT STATION NO.3 FOR SINGLE - SLOT INJECTION

JET REYNOLDS NUMBER, $Re_{t,j} = 1.9 \times 10^5$

JET VELOCITY, $V_j = 76$ FT/SEC

MEASURING STATION

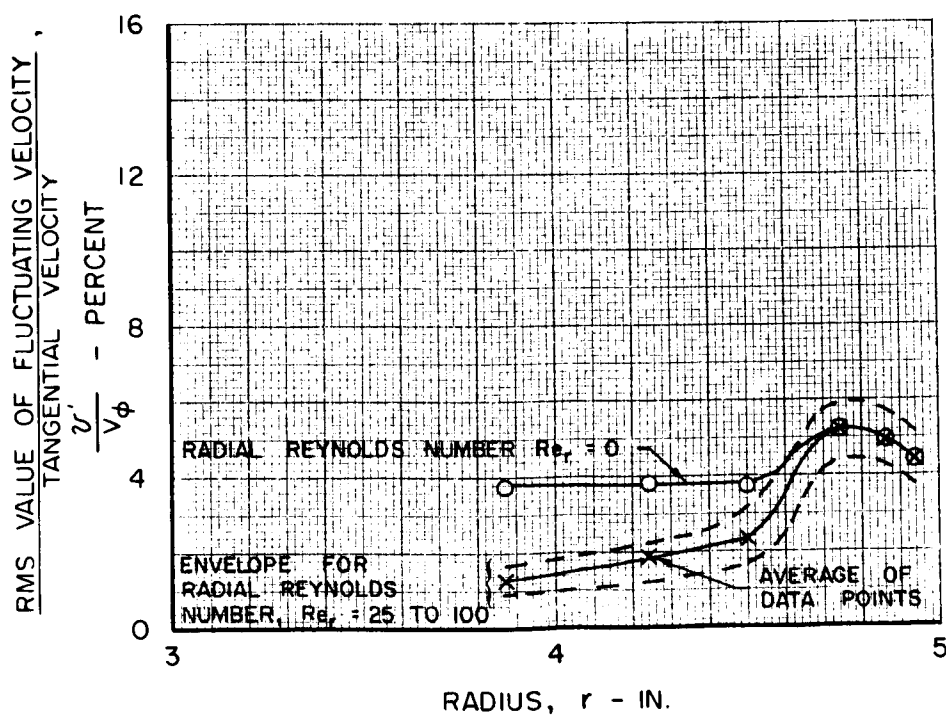
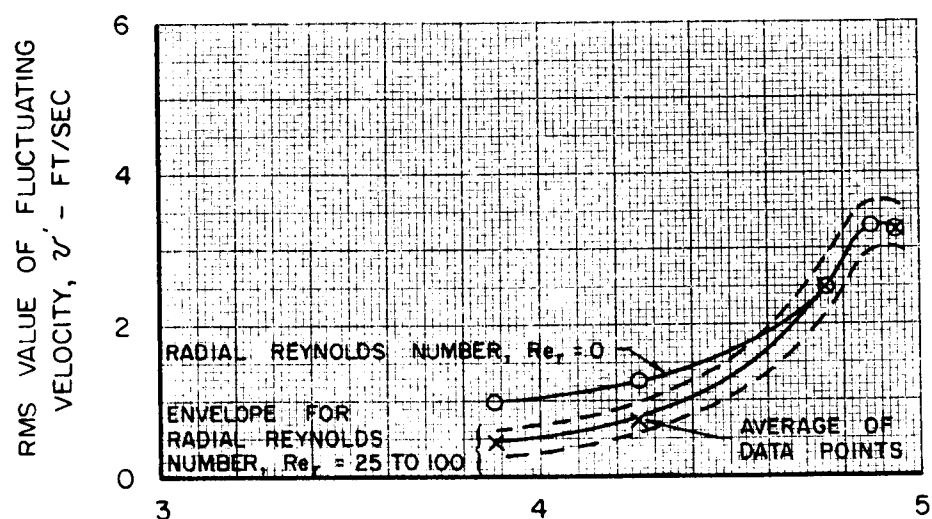
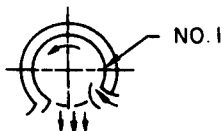


EFFECT OF RADIAL REYNOLDS NUMBER ON TURBULENCE INTENSITY PROFILES AT STATION NO. 1 FOR SINGLE-SLOT INJECTION

JET REYNOLDS NUMBER, $Re_{t,j} = 1.9 \times 10^5$

JET VELOCITY, $V_j = 76$ FT/SEC

MEASURING STATION

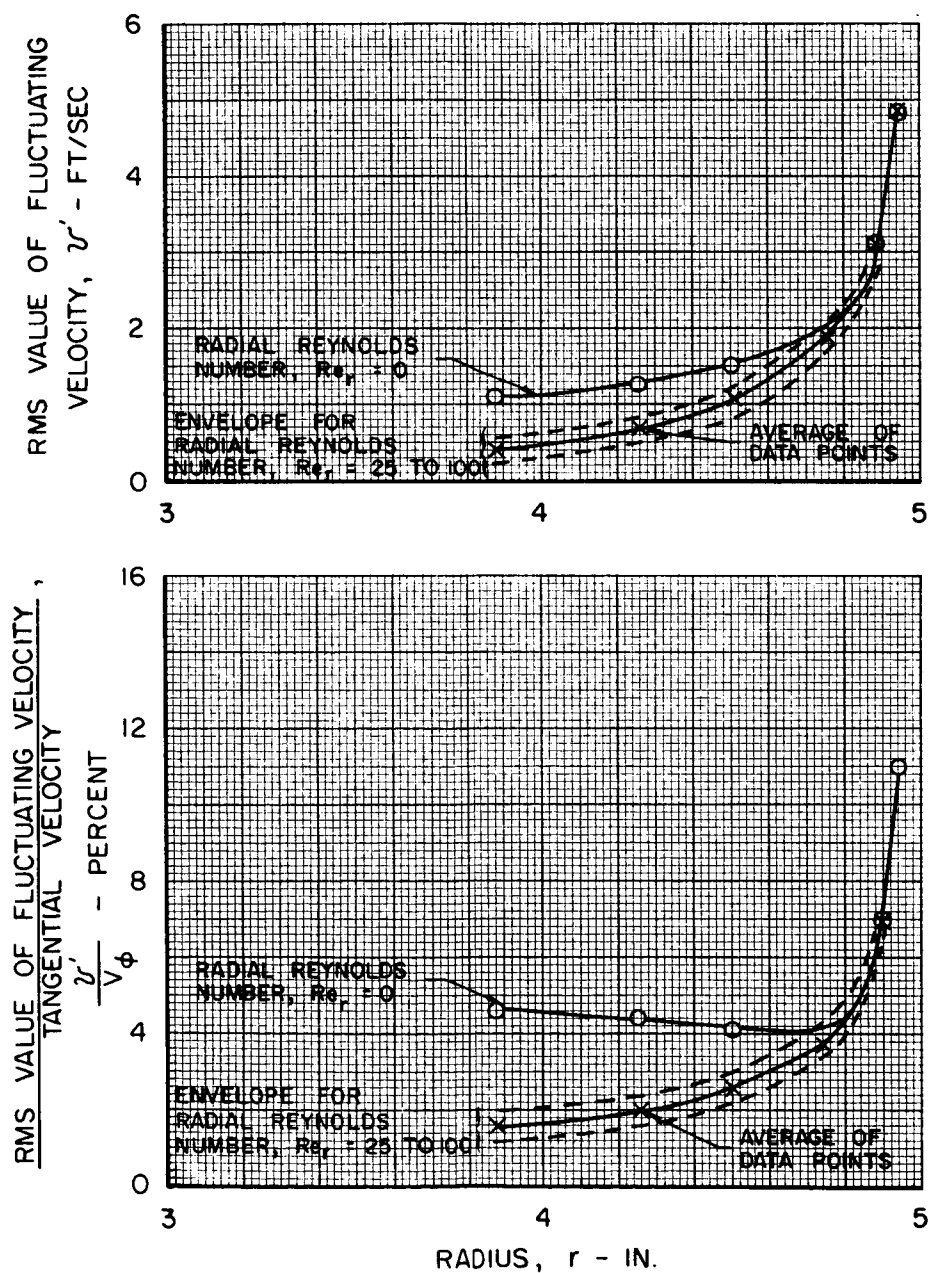
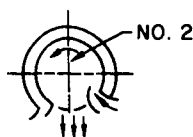


EFFECT OF RADIAL REYNOLDS NUMBER ON TURBULENCE INTENSITY PROFILES AT STATION NO.2 FOR SINGLE-SLOT INJECTION

JET REYNOLDS NUMBER, $Re_{t,j} = 1.9 \times 10^5$

JET VELOCITY, $V_j = 76$ FT/SEC

MEASURING STATION

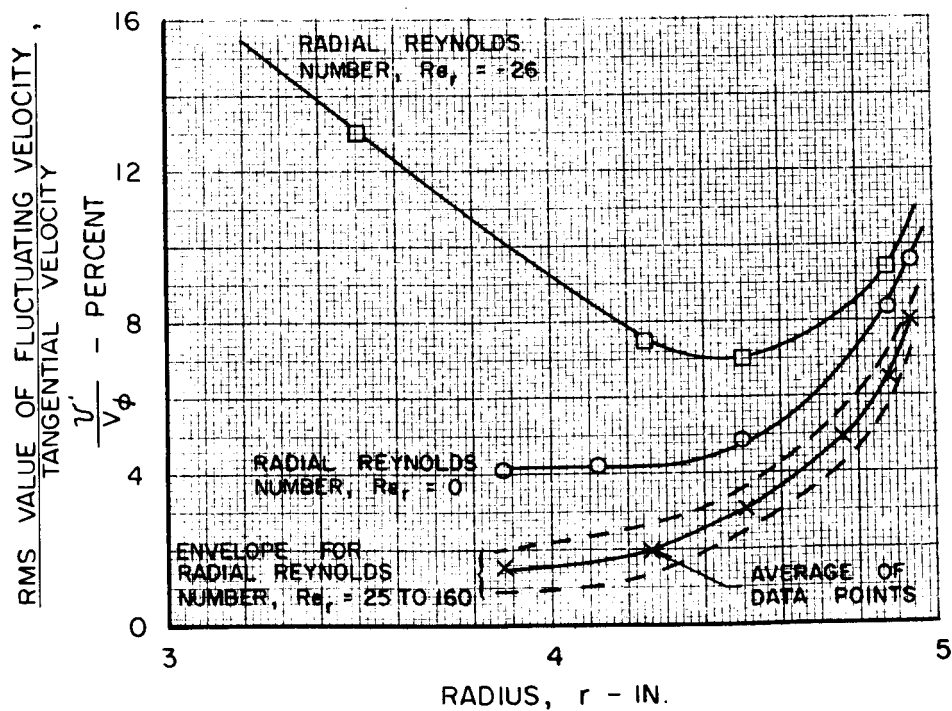
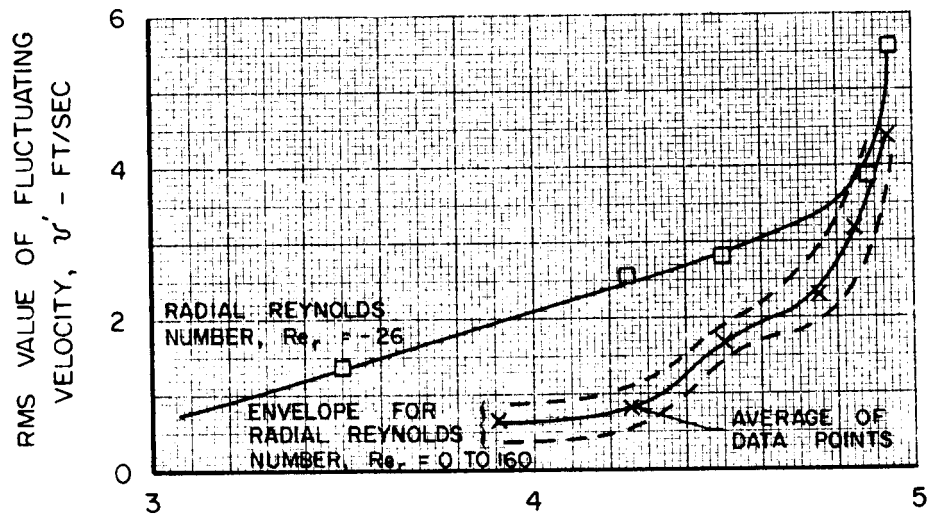
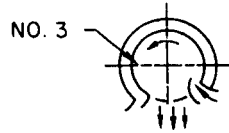


EFFECT OF RADIAL REYNOLDS NUMBER ON TURBULENCE INTENSITY PROFILES AT STATION NO. 3 FOR SINGLE-SLOT INJECTION

JET REYNOLDS NUMBER, $Re_{t,j} = 1.9 \times 10^5$

JET VELOCITY, $V_j = 76$ FT/SEC

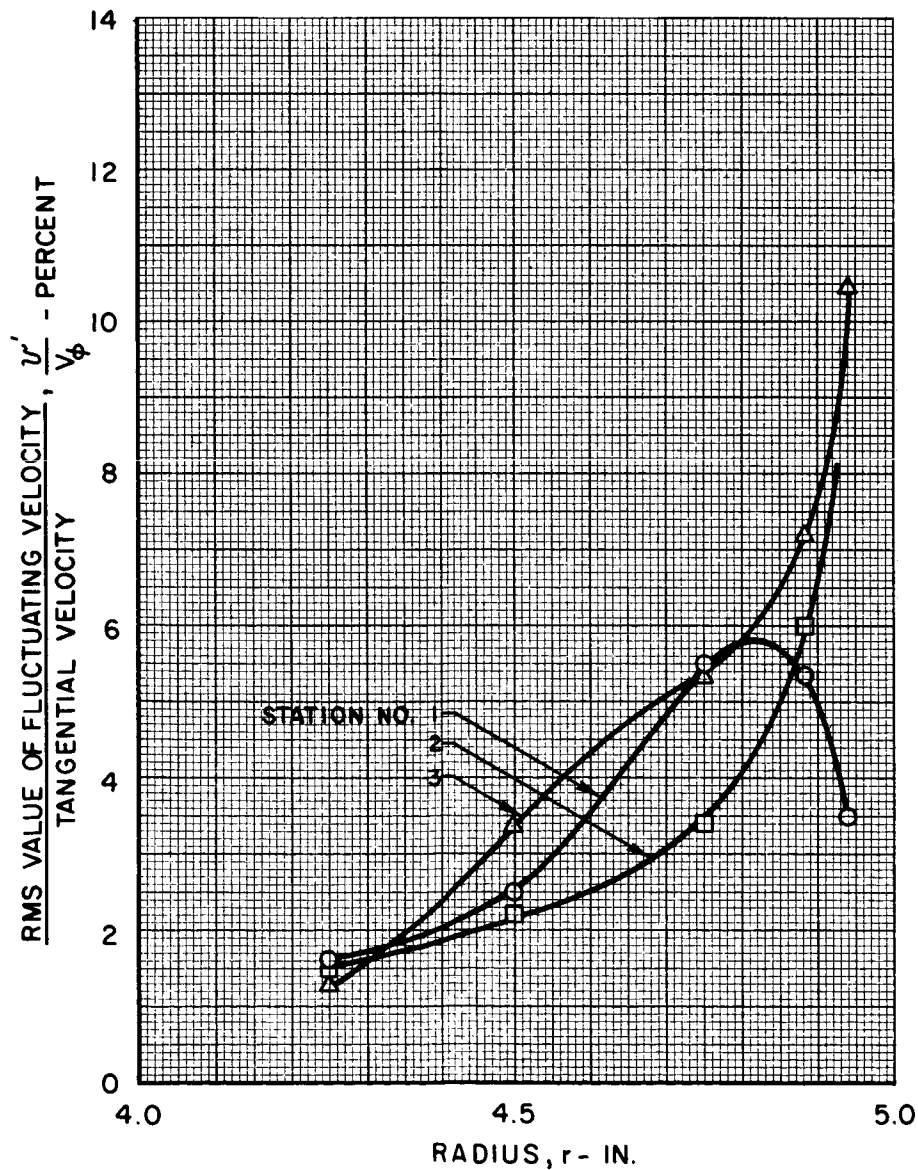
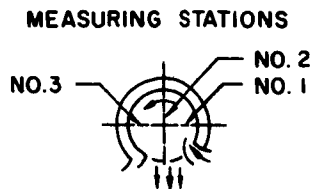
MEASURING STATION



COMPARISON OF TURBULENCE INTENSITY PROFILES AT STATIONS NO.1, NO.2, AND NO.3 FOR SINGLE-SLOT INJECTION AT RADIAL REYNOLDS NUMBER OF 100

JET REYNOLDS NUMBER, $Re_{t,j} = 1.9 \times 10^5$

JET VELOCITY, $V_j = 76$ FT/SEC

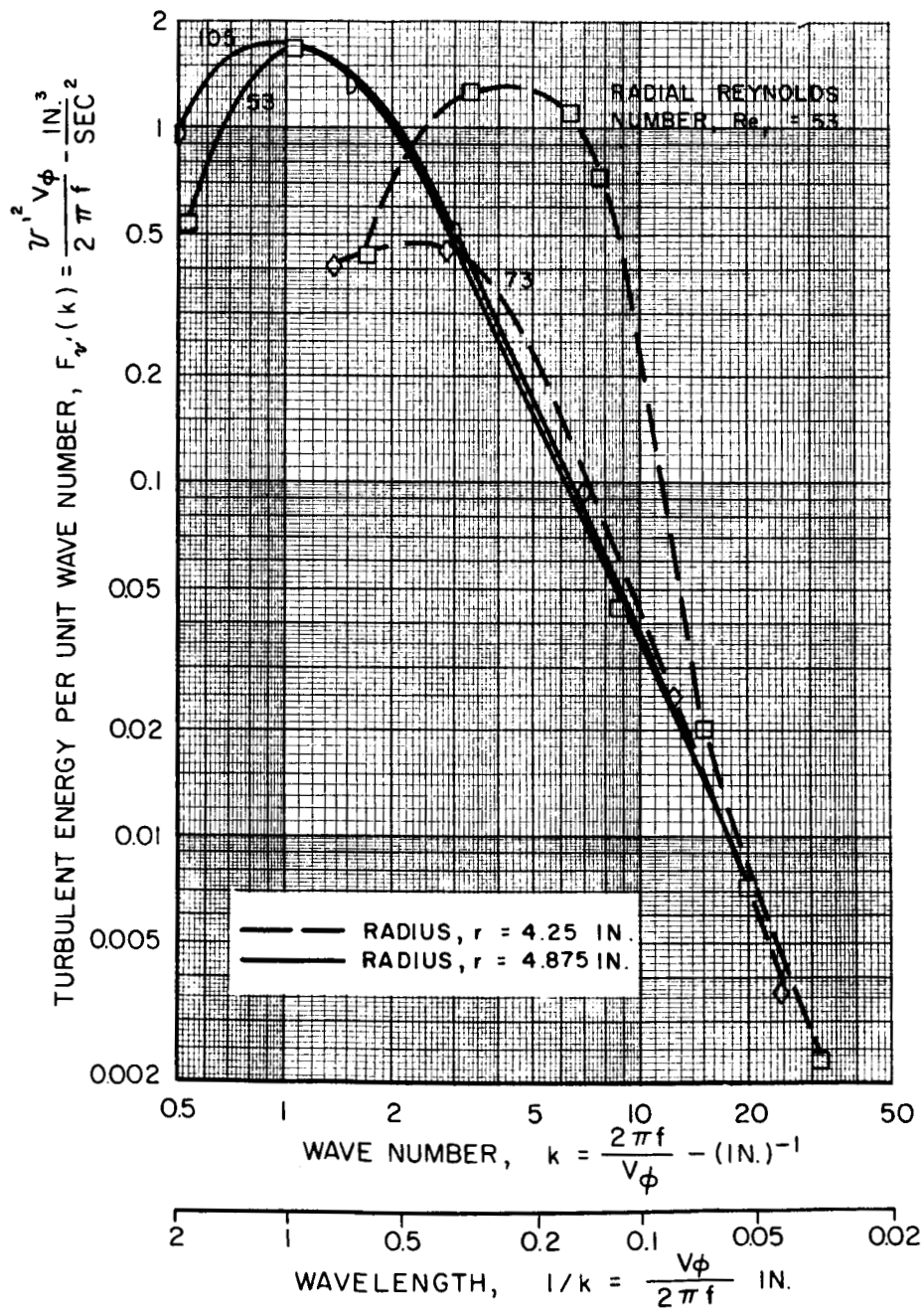
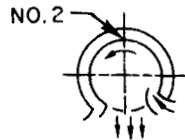


EFFECT OF RADIAL REYNOLDS NUMBER ON ENERGY SPECTRUM AT STATION NO.2 FOR SINGLE-SLOT INJECTION

JET REYNOLDS NUMBER, $Re_{t,j} = 1.9 \times 10^5$

JET VELOCITY, $V_j = 76$ FT/SEC

MEASURING STATION

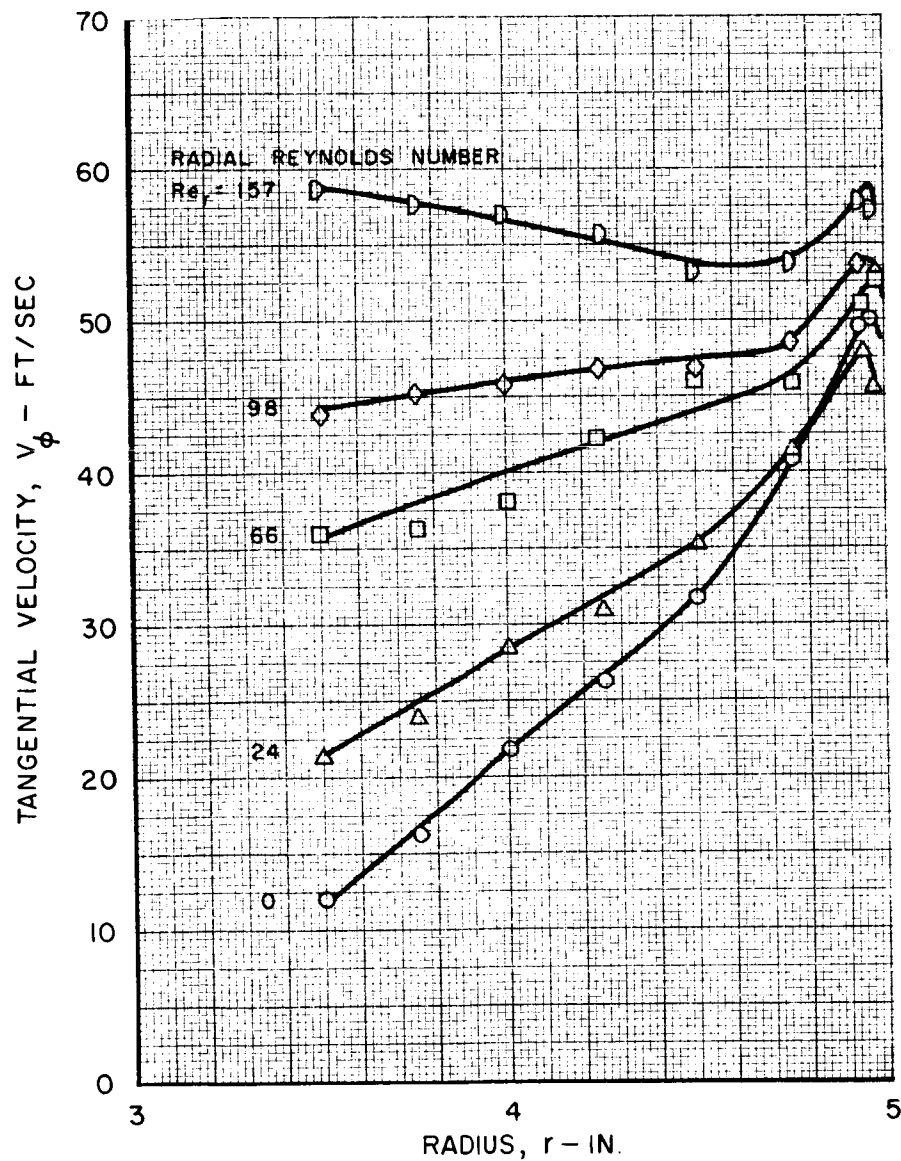
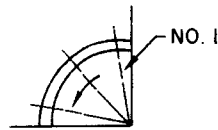


EFFECT OF RADIAL REYNOLDS NUMBER ON TANGENTIAL VELOCITY PROFILES AT STATION NO. 1 FOR 2144 - PORT INJECTION

JET REYNOLDS NUMBER, $Re_{t,j} = 2.2 \times 10^5$

JET VELOCITY, $V_j = 89$ FT/SEC

MEASURING STATION

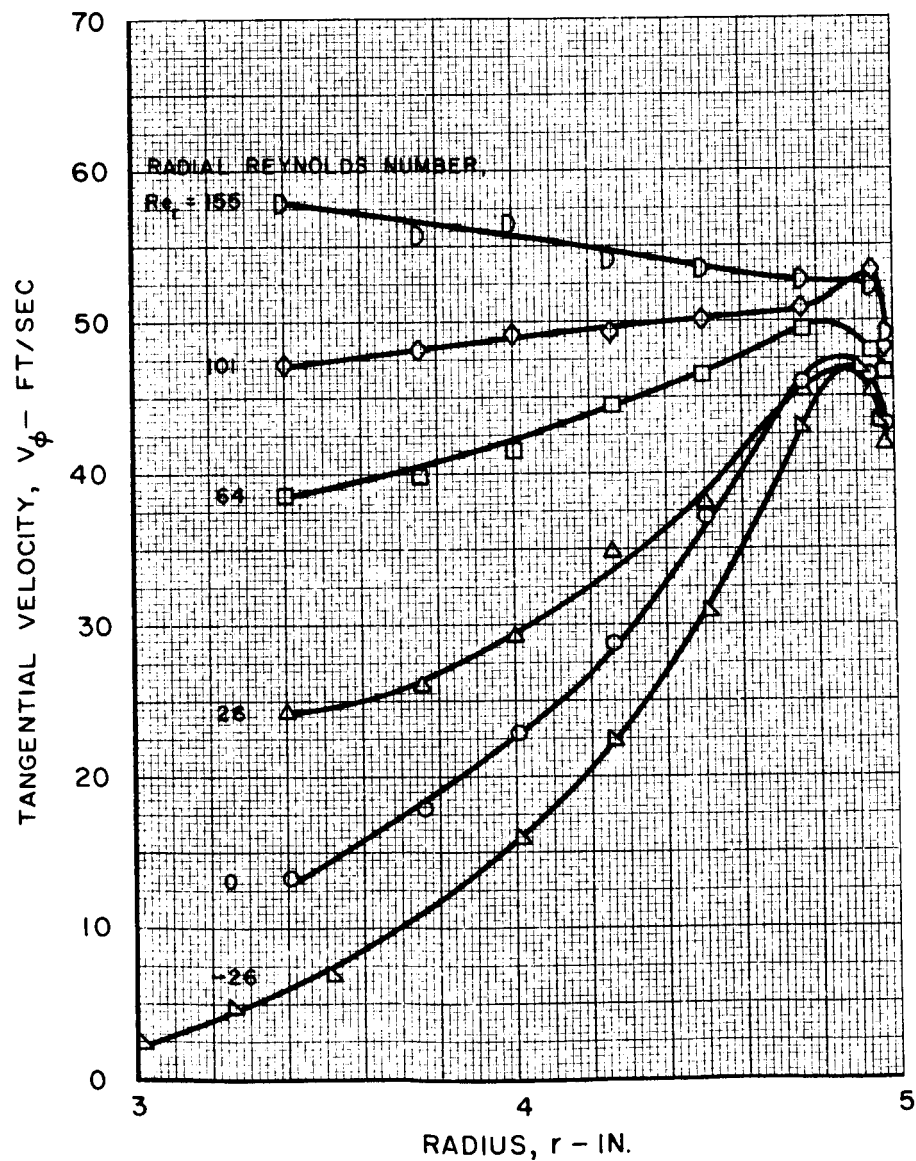
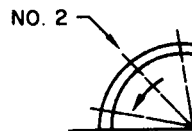


EFFECT OF RADIAL REYNOLDS NUMBER ON TANGENTIAL VELOCITY PROFILES AT STATION NO.2 FOR 2144 - PORT INJECTION

JET REYNOLDS NUMBER, $Re_{t,j} = 2.2 \times 10^5$

JET VELOCITY, $V_j = 89$ FT/SEC

MEASURING STATION

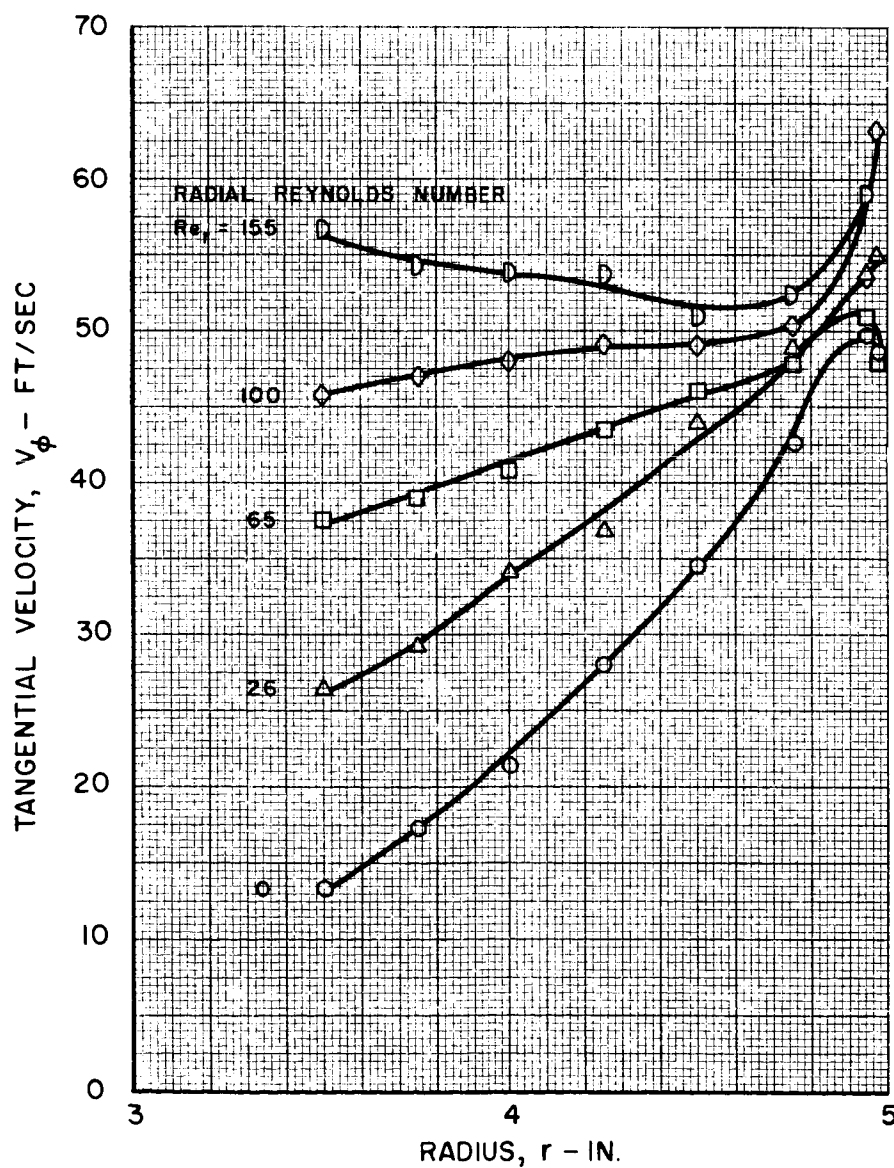
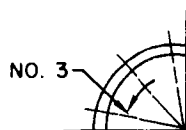


EFFECT OF RADIAL REYNOLDS NUMBER ON TANGENTIAL VELOCITY PROFILES AT STATION NO.3 FOR 2144 - PORT INJECTION

JET REYNOLDS NUMBER, $Re_{t,j} = 2.2 \times 10^5$

JET VELOCITY, $V_j = 89$ FT/SEC

MEASURING STATION

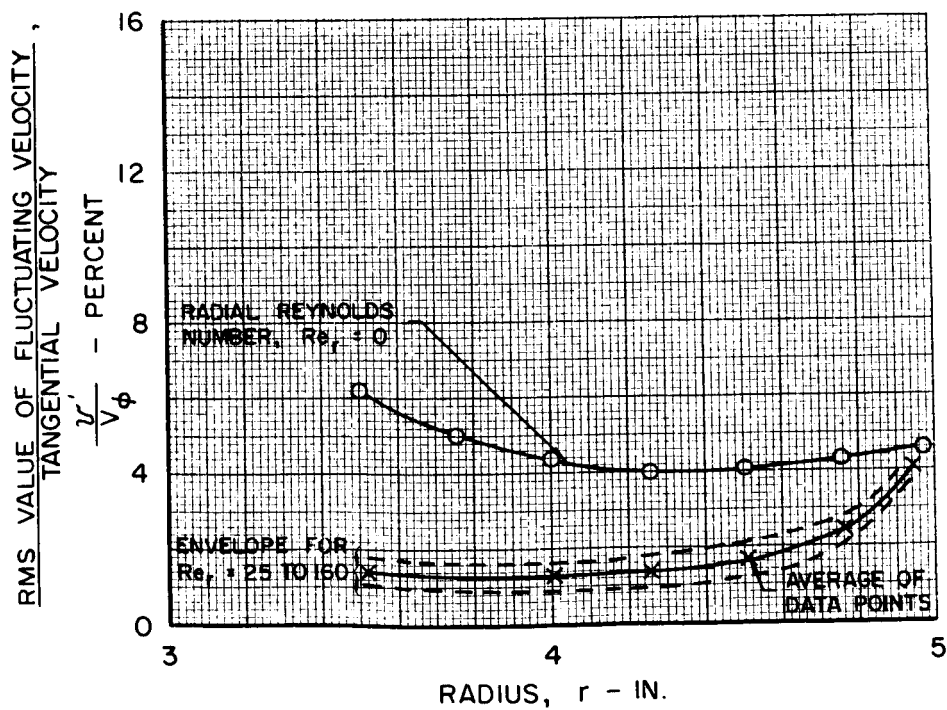
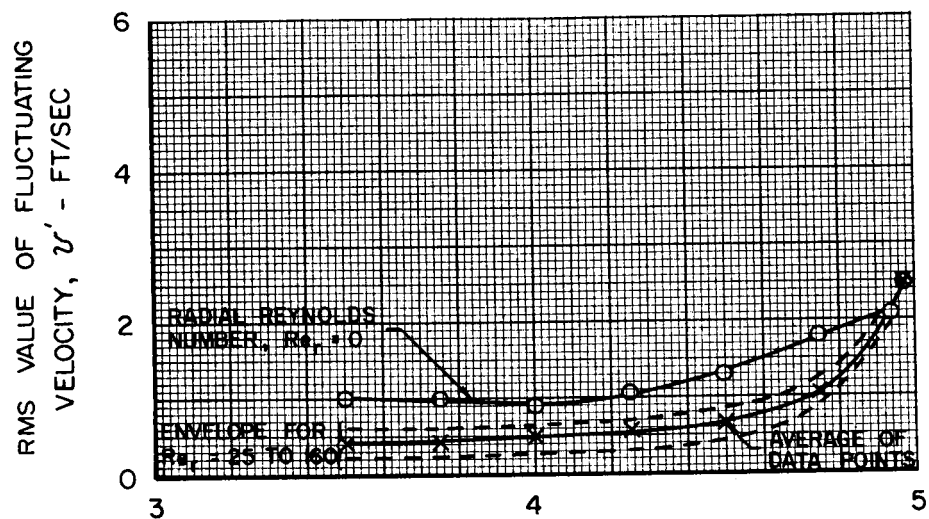
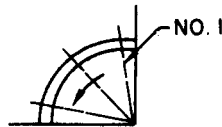


EFFECT OF RADIAL REYNOLDS NUMBER ON TURBULENCE INTENSITY PROFILES AT STATION NO. 1 FOR 2144-PORT INJECTION

JET REYNOLDS NUMBER, $Re_{t,j} = 2.2 \times 10^5$

JET VELOCITY, $V_j = 89$ FT/SEC

MEASURING STATION

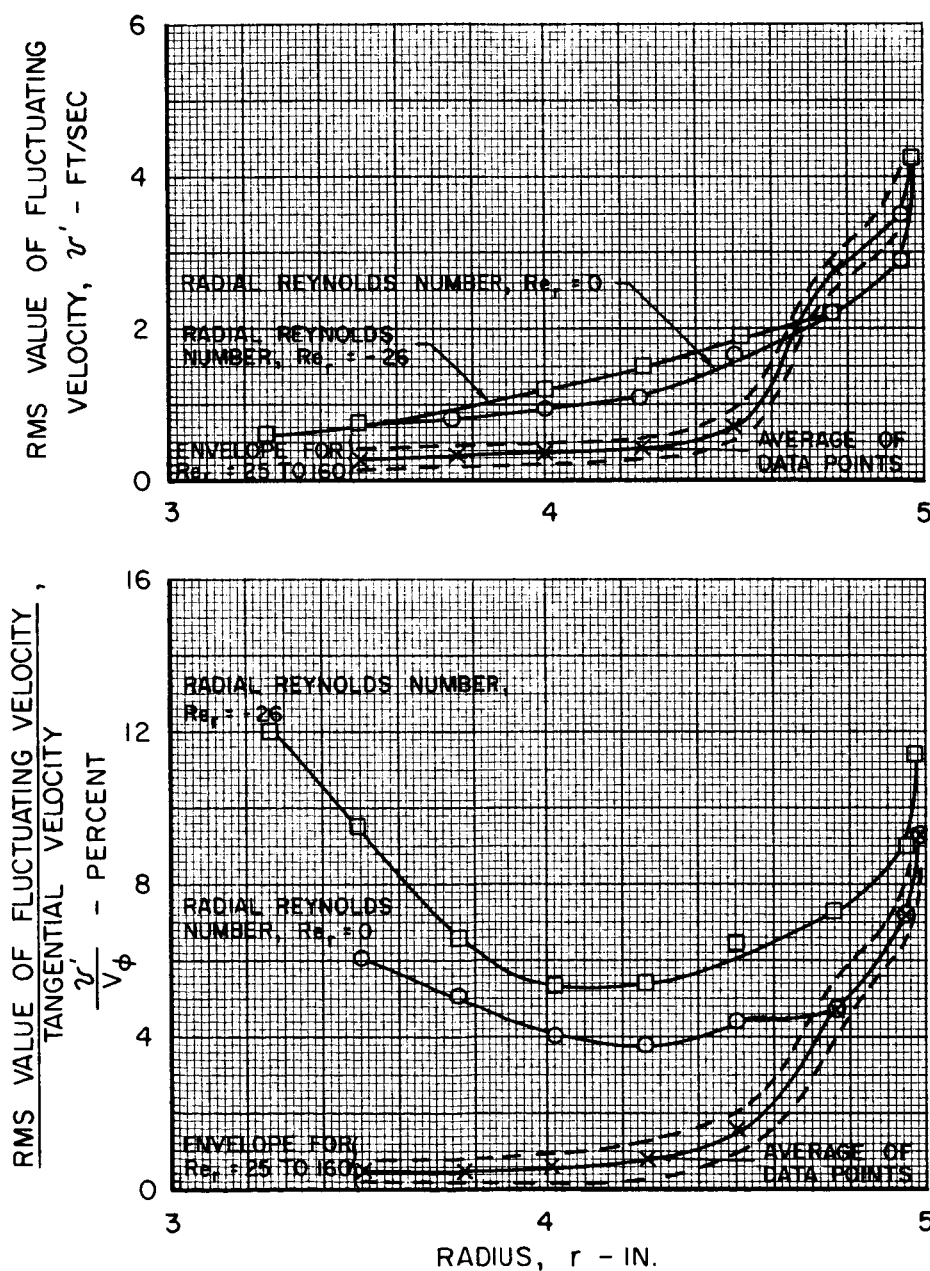
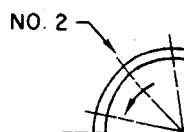


EFFECT OF RADIAL REYNOLDS NUMBER ON TURBULENCE INTENSITY PROFILES AT STATION NO.2 FOR 2144-PORT INJECTION

JET REYNOLDS NUMBER, $Re_{t,j} = 2.2 \times 10^5$

JET VELOCITY, $v_j = 89$ FT/SEC

MEASURING STATION

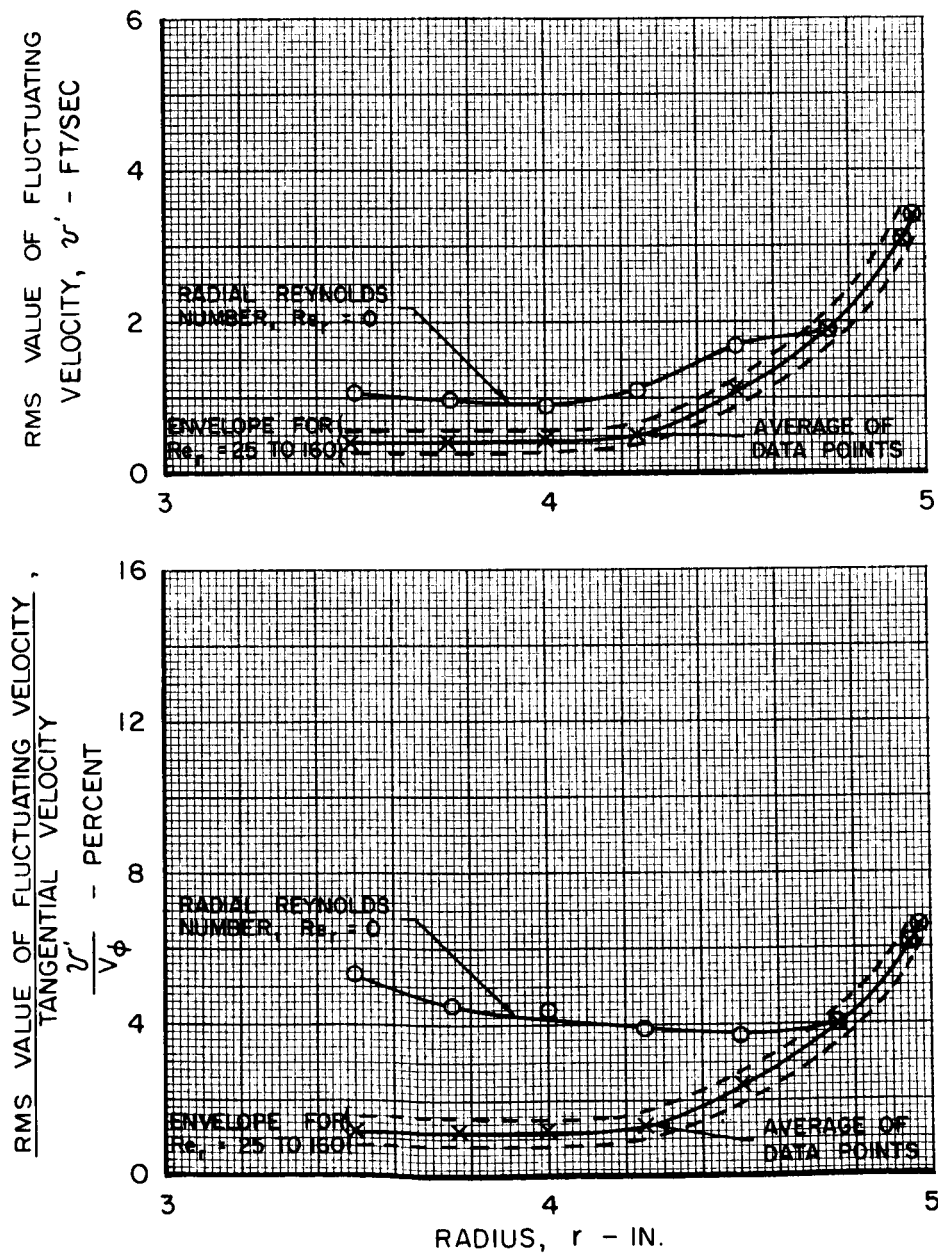
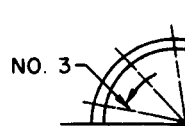


EFFECT OF RADIAL REYNOLDS NUMBER ON TURBULENCE INTENSITY PROFILES AT STATION NO.3 FOR 2144 - PORT INJECTION

JET REYNOLDS NUMBER, $Re_{t,j} = 2.2 \times 10^5$

JET VELOCITY, $V_j = 89$ FT/SEC

MEASURING STATION

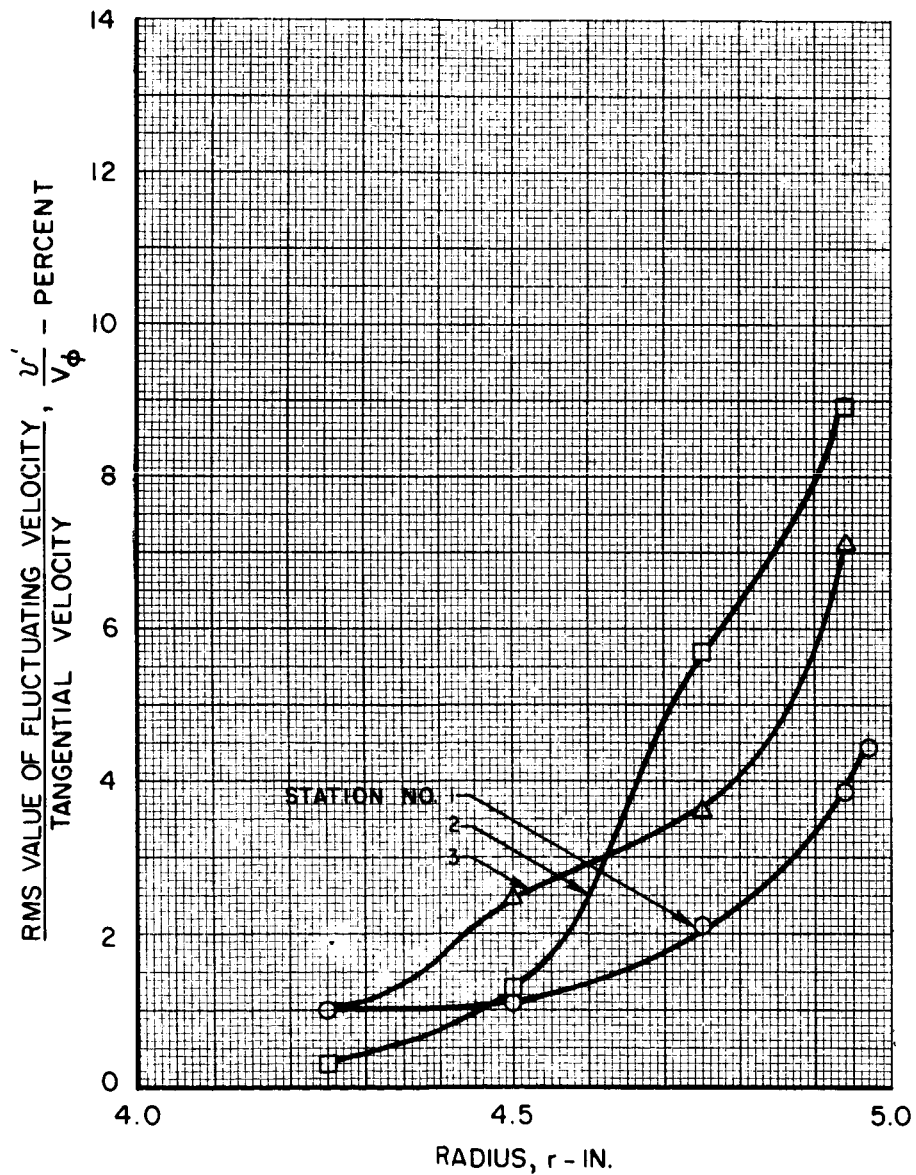


COMPARISON OF TURBULENCE INTENSITY PROFILES AT STATIONS NO.1, NO.2, AND NO.3 FOR 2144-PORT INJECTION AT RADIAL REYNOLDS NUMBER OF 100

JET REYNOLDS NUMBER, $Re_{t,j} = 2.2 \times 10^5$

JET VELOCITY, $V_j = 89$ FT/SEC

MEASURING STATIONS

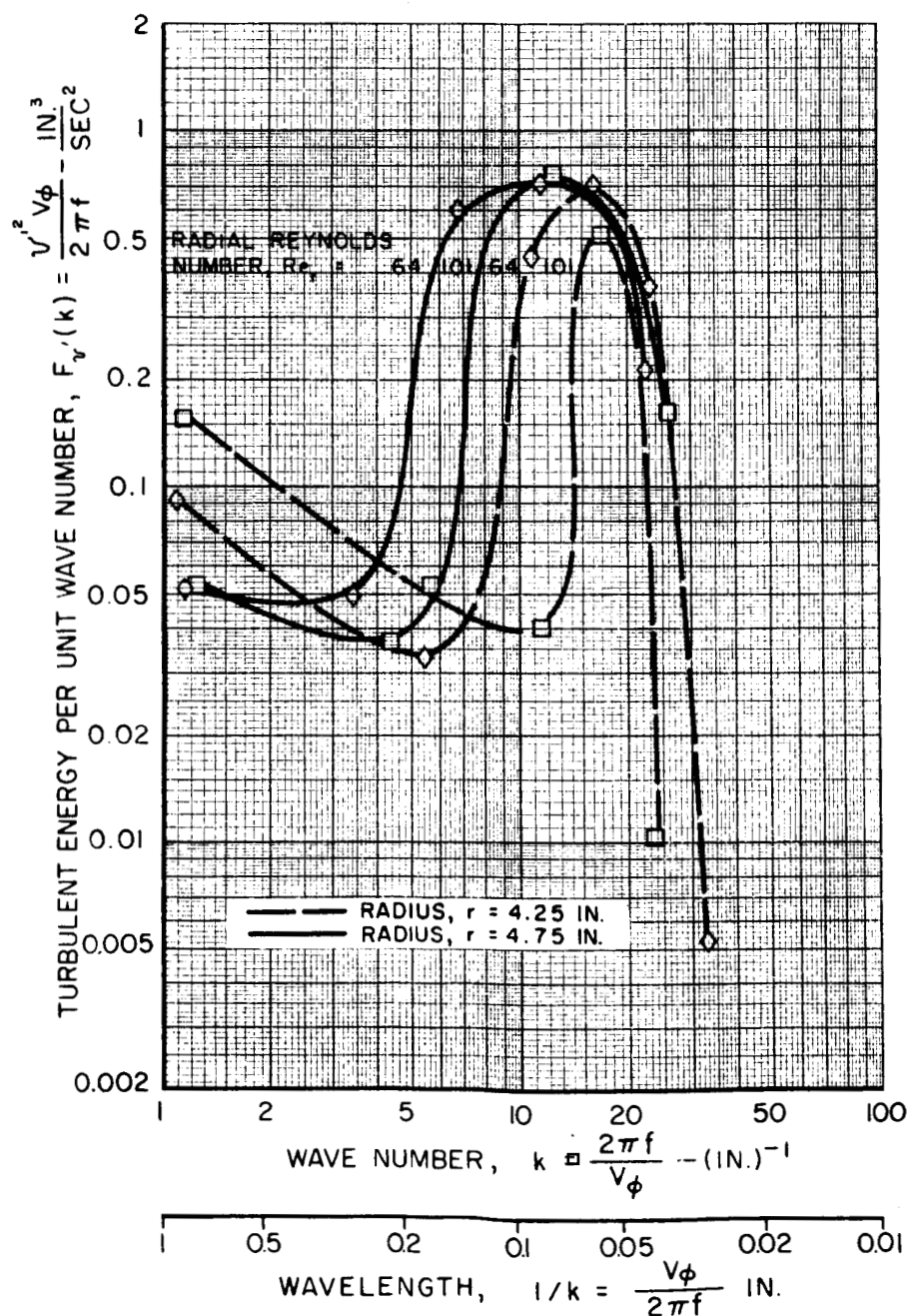
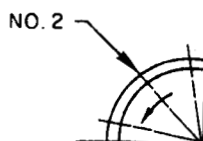


EFFECT OF RADIAL REYNOLDS NUMBER ON ENERGY SPECTRUM AT STATION NO. 2 FOR 2144 - PORT INJECTION



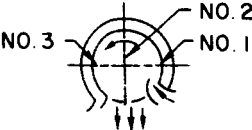
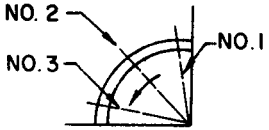
JET REYNOLDS NUMBER, $Re_{t,j} = 2.2 \times 10^5$

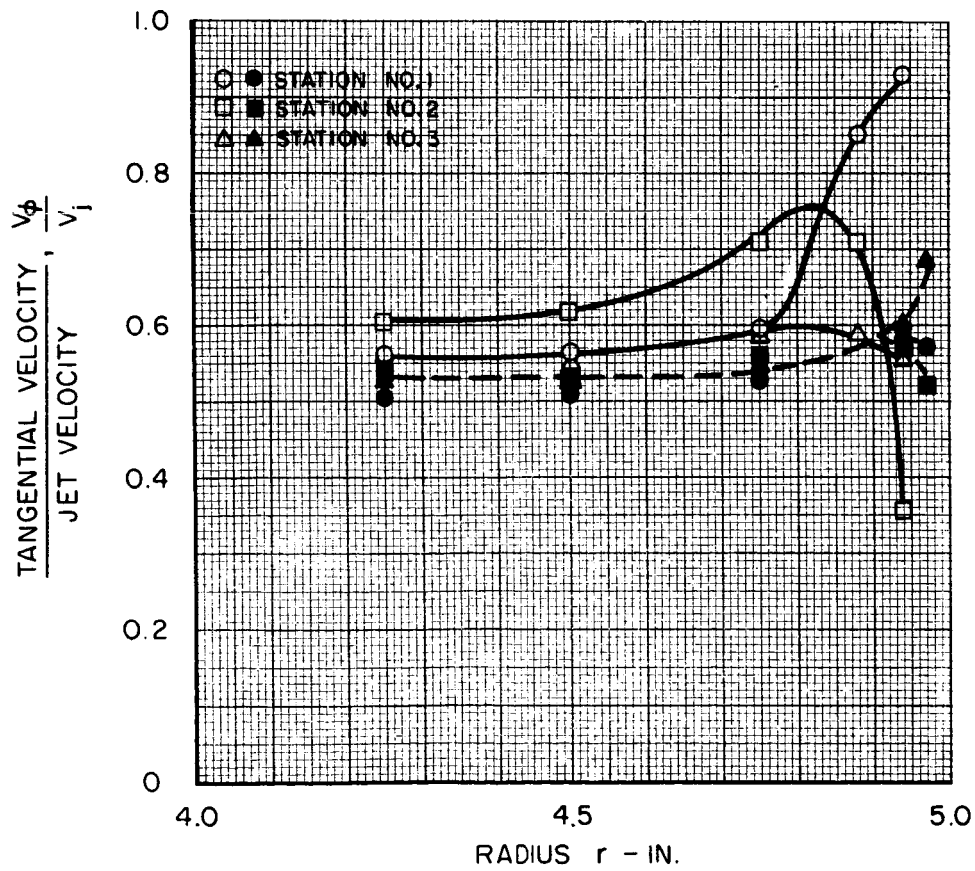
JET VELOCITY, $V_j = 89$ FT/SEC

MEASURING STATION



COMPARISON OF SINGLE - SLOT - INJECTION
AND 2144 - PORT-INJECTION TANGENTIAL VELOCITY
PROFILES AT RADIAL REYNOLDS NUMBER OF 100

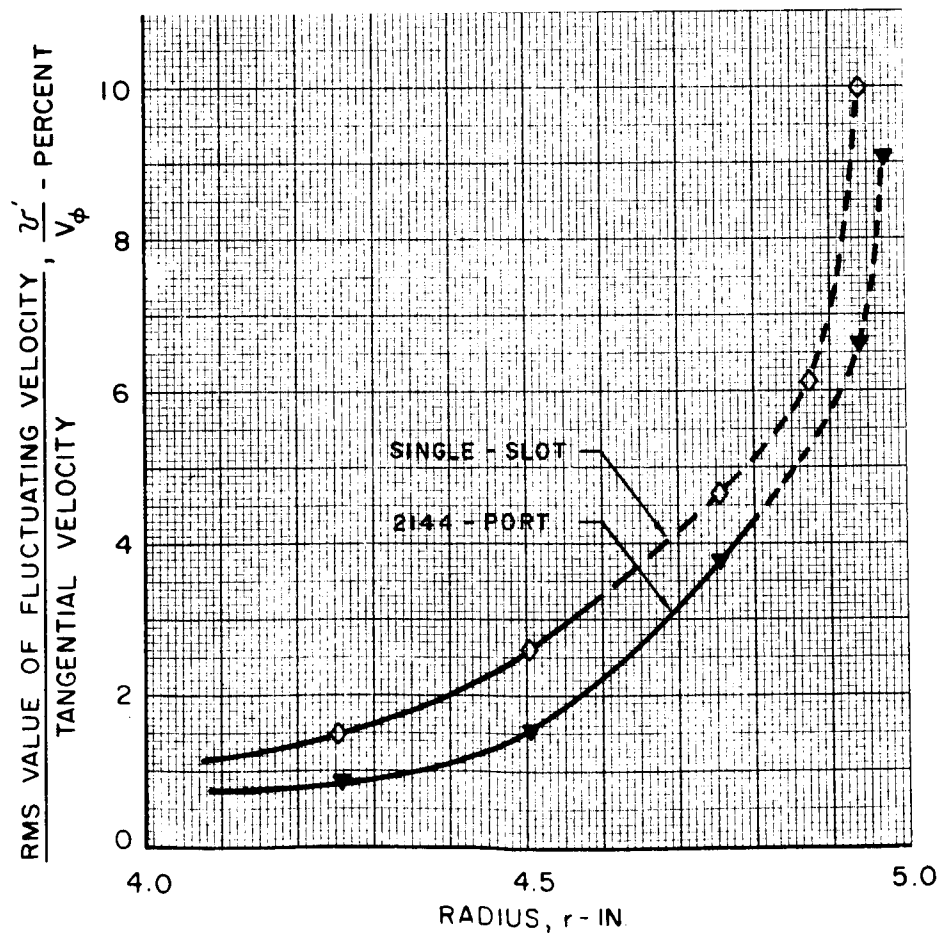
CURVE		
INJECTION CONFIGURATION	SINGLE - SLOT	2144 - PORT
JET VELOCITY, V_j	76 FT/SEC	89 FT/SEC
MASS FLOW	0.23 LB/SEC	0.20 LB/SEC
JET REYNOLDS NUMBER, $Re_{t,j}$	1.9×10^5	2.2×10^5
MEASURING STATIONS		



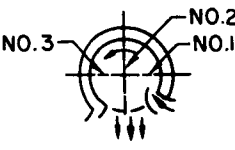
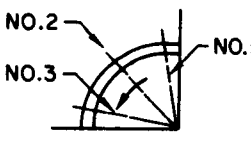
COMPARISON OF AVERAGE SINGLE-SLOT-INJECTION AND 2144-PORT-INJECTION TURBULENCE INTENSITY PROFILES AT RADIAL REYNOLDS NUMBER OF 100

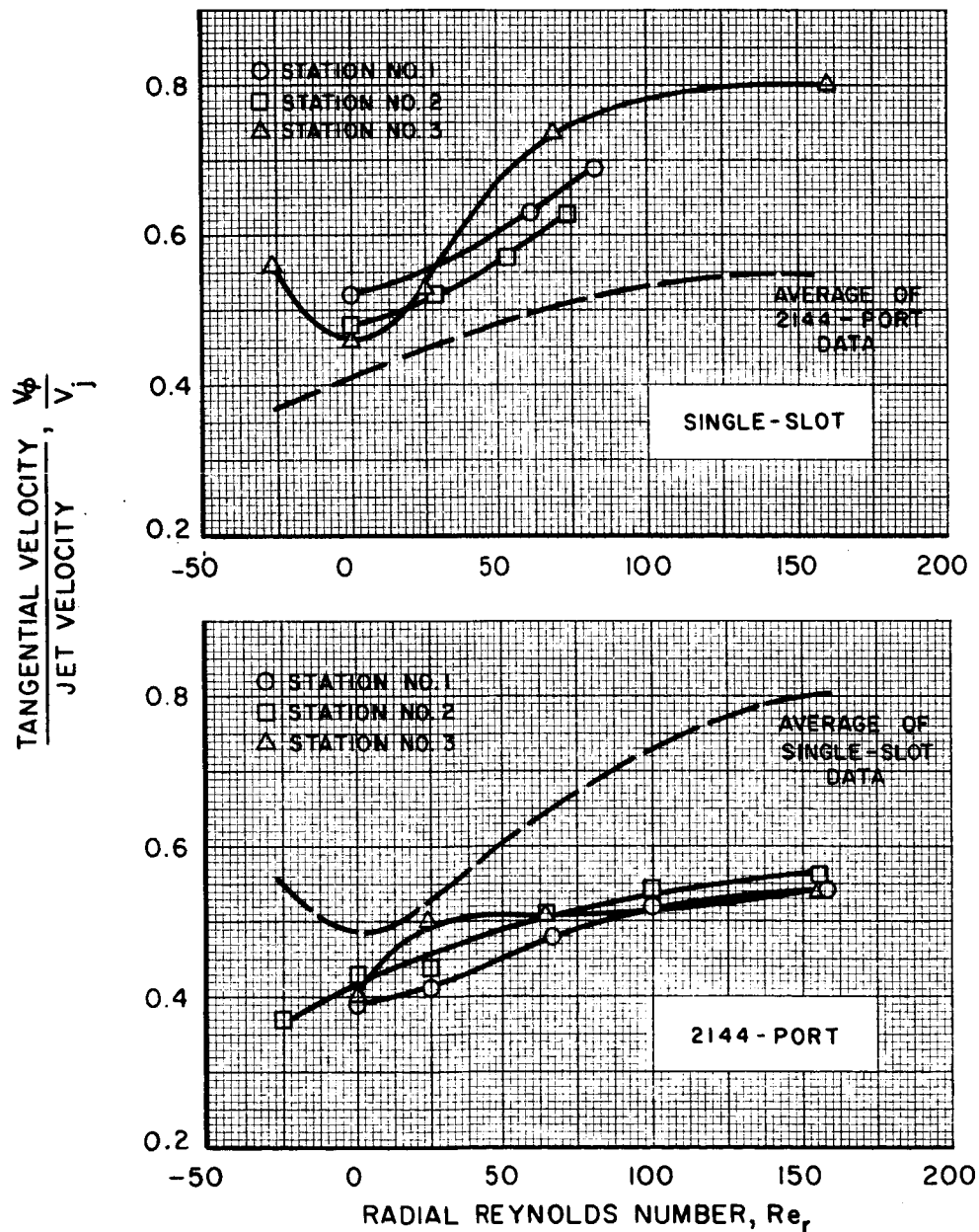
NOTE: CURVES ARE BASED ON ARITHMETIC AVERAGE OF DATA FOR THREE MEASURING STATIONS PRESENTED IN FIGS. 13 AND 21
DASHED LINE INDICATES REGION OF BOUNDARY LAYER

INJECTION CONFIGURATION	SINGLE-SLOT	2144-PORT
JET VELOCITY, V_j	76 FT/SEC	89 FT/SEC
JET REYNOLDS NUMBER, $Re_{t,j}$	1.9×10^5	2.2×10^5





EFFECT OF RADIAL REYNOLDS NUMBER ON TANGENTIAL VELOCITY FOR SINGLE-SLOT INJECTION AND 2144-PORT INJECTION AT A RADIUS OF 4.5 IN.

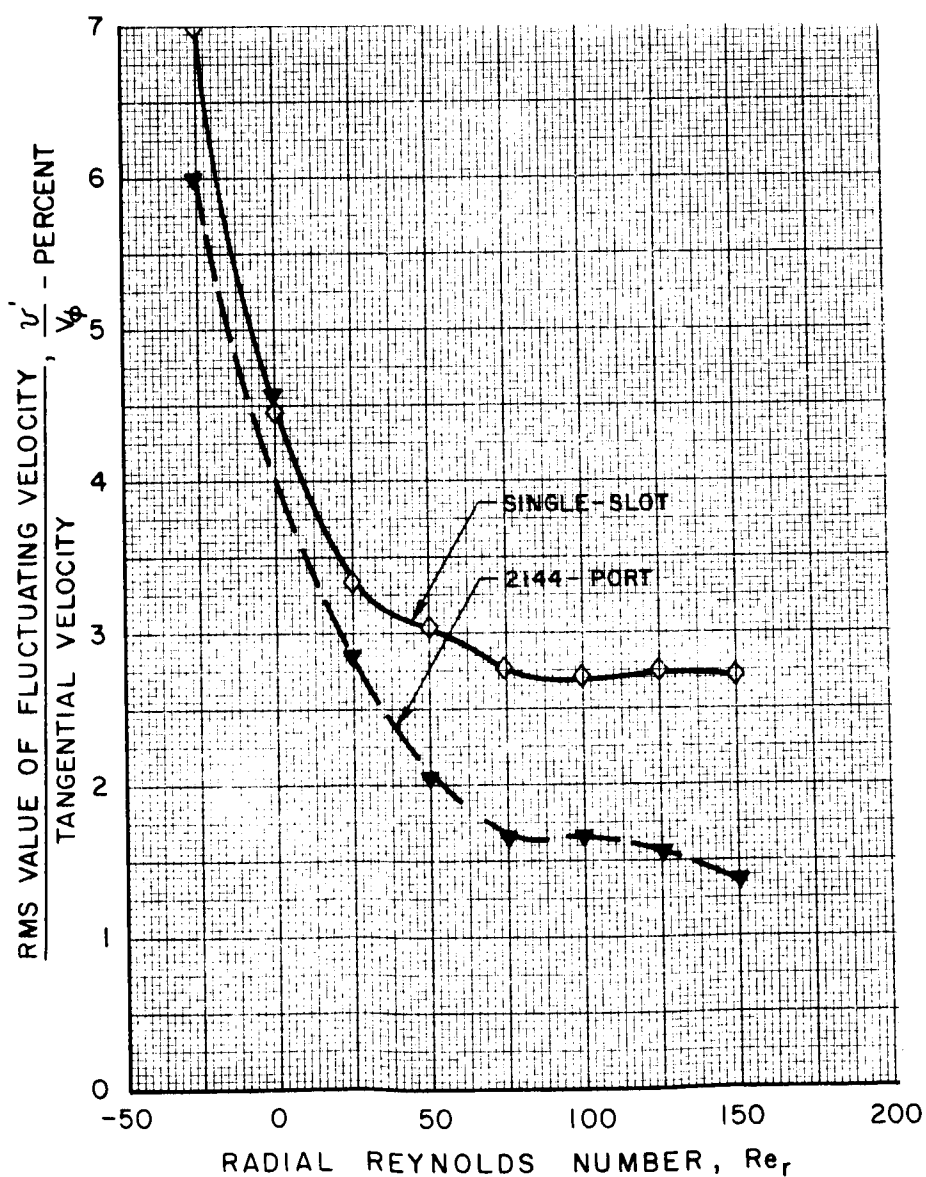
INJECTION CONFIGURATION	SINGLE - SLOT	2144 - PORT
JET VELOCITY, V_j	76 FT/SEC	89 FT/SEC
JET REYNOLDS NUMBER, $Re_{t,j}$	1.9×10^5	2.2×10^5
MEASURING STATIONS		





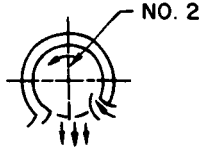
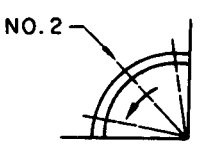
EFFECT OF RADIAL REYNOLDS NUMBER ON TURBULENCE INTENSITY AT RADIUS OF 4.5 IN. FOR SINGLE-SLOT INJECTION AND 2144-PORT INJECTION

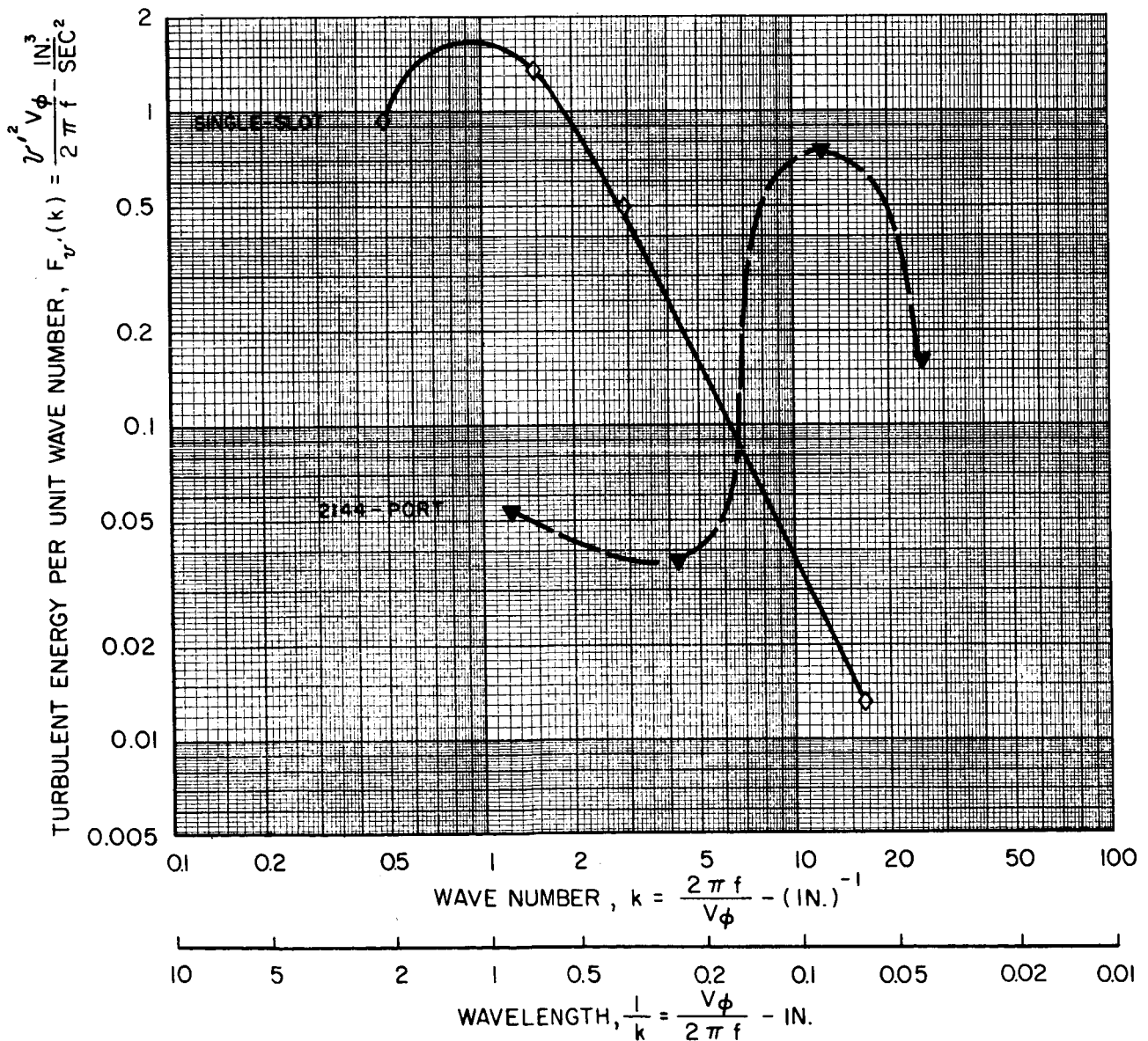
NOTE: CURVES ARE BASED ON ARITHMETIC AVERAGE OF DATA FOR THREE MEASURING STATIONS

CURVE		
INJECTION CONFIGURATION	SINGLE-SLOT	2144-PORT
JET VELOCITY, V_j	76 FT/SEC	89 FT/SEC
JET REYNOLDS NUMBER, $Re_{t,j}$	1.9×10^5	2.2×10^5

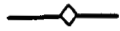


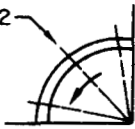


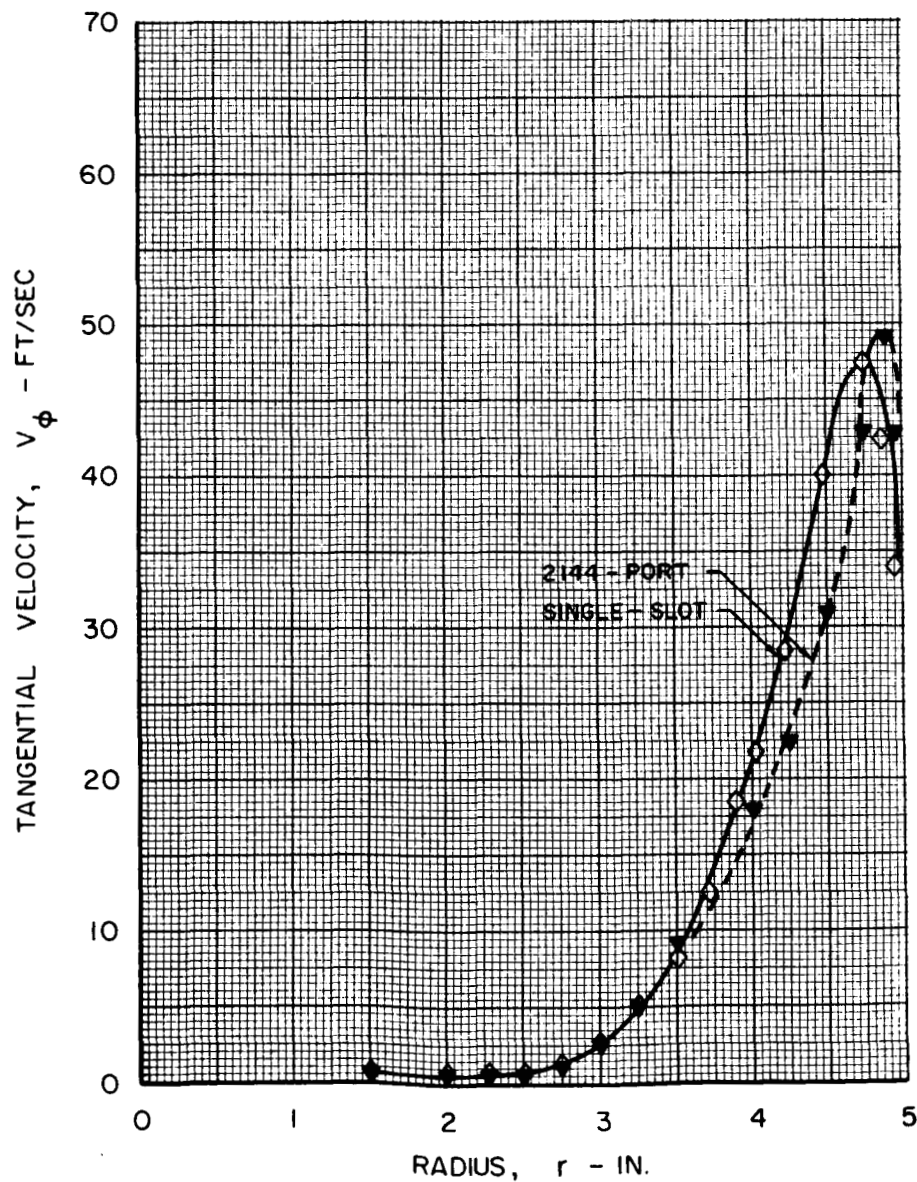
**COMPARISON OF SINGLE-SLOT INJECTION AND 2144-PORT INJECTION
ENERGY SPECTRA AT STATION NO.2, RADIUS OF 4.75 IN.,
AND RADIAL REYNOLDS NUMBER OF 100**

CURVE		
INJECTION CONFIGURATION	SINGLE-SLOT	2144-PORT
JET VELOCITY, V_j	76 FT/SEC	89 FT/SEC
JET REYNOLDS NUMBER, $Re_{t,j}$	1.9×10^5	2.2×10^5
MEASURING STATION		






**COMPARISON OF TYPICAL SINGLE - SLOT - INJECTION
AND 2144 - PORT - INJECTION TANGENTIAL VELOCITY PROFILES
AT RADIAL REYNOLDS NUMBER OF -26**

CURVE		
INJECTION CONFIGURATION	SINGLE - SLOT	2144 - PORT
JET VELOCITY, V_j	76 FT/SEC	89 FT/SEC
JET REYNOLDS NUMBER, $Re_{t,j}$	1.9×10^5	2.2×10^5
MEASURING STATION	NO. 3 	NO. 2 



**COMPARISON OF TYPICAL SINGLE - SLOT - INJECTION
AND 2144 - PORT - INJECTION TURBULENCE INTENSITY PROFILES
AT RADIAL REYNOLDS NUMBER OF -26**

CURVE		
INJECTION CONFIGURATION	SINGLE - SLOT	2144 - PORT
JET VELOCITY, V_j	76 FT/SEC	89 FT/SEC
JET REYNOLDS NUMBER, $Re_{f,j}$	1.9×10^5	2.2×10^5
MEASURING STATION	NO. 3 	NO. 2 